

Articles

Toward Highly Metallized Polymers: Synthesis and Characterization of Silicon-Bridged [1]Ferrocenophanes with Pendent Cluster Substituents

Wing Yan Chan, Andrea Berenbaum, Scott B. Clendenning, Alan J. Lough, and Ian Manners*

Department of Chemistry, University of Toronto, 80 St. George Street, Toronto, Ontario, Canada, M5S 3H6

Received May 12, 2003

The acetylide-substituted sila[1]ferrocenophanes $[\text{Fe}(\eta\text{-C}_5\text{H}_4)_2\text{Si}(\text{Me})\text{C}\equiv\text{CR}]$ ($\text{R} = \text{Ph}$ (**2a**), ^nBu (**2b**)) reacted with $[\text{Co}_2(\text{CO})_8]$, $[\{\text{MoCp}(\text{CO})_2\}_2]$, or $[\text{Ni}(\text{cod})_2]/\text{L}$ selectively at the triple bond to give pendent organocobalt $[\text{Fe}(\eta\text{-C}_5\text{H}_4)_2\text{Si}(\text{Me})\{\text{Co}_2(\text{CO})_6\text{C}_2\text{R}\}]$ ($\text{R} = \text{Ph}$ (**4a**), ^nBu (**4b**)) or organomolybdenum $[\text{Fe}(\eta\text{-C}_5\text{H}_4)_2\text{Si}(\text{Me})\{\text{Mo}_2\text{Cp}_2(\text{CO})_4\text{C}_2\text{Ph}\}]$ (**9**) clusters or mononuclear organonickel $[\text{Fe}(\eta\text{-C}_5\text{H}_4)_2\text{Si}(\text{Me})\{\text{Ni}(\text{L})\text{C}_2\text{Ph}\}]$ ($\text{L} = \text{dmpe}$ (**11**), $\text{L} = \text{dppe}$ (**12**)) complexes. The bis(acetylide)-substituted sila[1]ferrocenophanes $[\text{Fe}(\eta\text{-C}_5\text{H}_4)_2\text{Si}(\text{C}\equiv\text{CR})_2]$ ($\text{R} = ^n\text{Bu}$ (**6a**), Ph (**6b**)) reacted with $[\text{Co}_2(\text{CO})_8]$ in an analogous fashion, forming the novel pentametallic silicon-bridged [1]ferrocenophanes with two pendent cobalt clusters $[\text{Fe}(\eta\text{-C}_5\text{H}_4)_2\text{Si}\{\text{Co}_2(\text{CO})_6\text{C}_2\text{R}\}_2]$ ($\text{R} = ^n\text{Bu}$ (**7a**), $\text{R} = \text{Ph}$ (**7b**)). Compound **7b** subsequently underwent rapid hydrolytic ring-opening to yield an unusual, highly metallized silanol, $[(\eta\text{-C}_5\text{H}_5)\text{Fe}(\eta\text{-C}_5\text{H}_4)\text{-Si}(\text{OH})\{\text{Co}_2(\text{CO})_6\text{C}_2\text{Ph}\}_2]$ (**8b**). This reaction was found to be much slower for the hexynyl analogue (**7a**). The organonickel complexes (**11** and **12**) described in this work represent the first examples of mononuclear complexes prepared directly from an alkyne and $[\text{Ni}(\text{cod})_2]$. We postulate that steric factors prevent the addition of a second nickel fragment to the alkyne. The synthesis of a sila[1]ferrocenophane with a pendent platinum moiety was also attempted. However, reaction of **2a** with $[\text{Pt}(\text{PET}_3)_3]$ instead gave the platinasila[2]-ferrocenophane $[\text{Fe}(\eta\text{-C}_5\text{H}_4)_2\text{Pt}(\text{PET}_3)_2\text{Si}(\text{Me})\text{C}\equiv\text{CPh}]$ (**15**) via oxidative insertion of the platinum(0) fragment into a strained *ipso*-cyclopentadienyl carbon–silicon bond of the sila[1]ferrocenophane.

Introduction

Polymers containing metal atoms as part of the main chain or side group structure are attracting increasing attention as they offer potential access to new functional macromolecular and supramolecular materials with novel properties.^{1,2} For example, the presence of transition metal centers in a polymer allows redox control of the size and shape of a macroscopic object;³ the “wiring” of enzymes to electrodes;⁴ selective binding and sensing;⁵ the generation of liquid crystallinity,⁶ magnetic nanoparticle composites,⁷ supramolecular materials,⁸ and a wide variety of other desirable physical and

chemical characteristics.^{1,2} However, despite the significant expansion of the metallopolymer area over the past decade or so, most materials reported to date still contain relatively low concentrations of metal atoms.

Metal cluster complexes exhibit many useful catalytic, optical, and other potentially useful properties for materials science applications.⁹ The incorporation of these remarkable metallo units into high molecular weight, processable polymers clearly offers exciting

* Corresponding author. E-mail: imanners@alchemy.chem.utoronto.ca. Fax: (416) 978-6157.

(1) (a) Archer, R. D. *Inorganic and Organometallic Polymers*; John Wiley & Sons Inc.: New York, 2001. (b) Manners, I. *Science* **2001**, *294*, 1664–1666.

(2) (a) Schubert, U. S.; Heller, M. *Chem. Eur. J.* **2001**, *7*, 5252–5259. (b) Nguyen, P.; Gómez-Eliphe, P.; Manners, I. *Chem. Rev.* **1999**, *99*, 1515–1548.

(3) (a) Yoshida, R.; Takahashi, T.; Yamaguchi, T.; Ichijo, H. *Adv. Mater.* **1997**, *9*, 175–178. (b) Arsénault, A. C.; Miguez, H.; Kitaev, V.; Ozin, G. A.; Manners, I. *Adv. Mater.* **2003**, *15*, 503–507.

(4) Caruana, D. J.; Heller, A. *J. Am. Chem. Soc.* **1999**, *121*, 769–774.

(5) (a) McQuade, D. T.; Pullen, A. E.; Swager, T. M. *Chem. Rev.* **2000**, *100*, 2537–2574. (b) Wang, Z.; McWilliams, A. R.; Evans, C. E. B.; Lu, X.; Chung, S.; Winnik, M. A.; Manners, I. *Adv. Funct. Mater.* **2002**, *12*, 415–419.

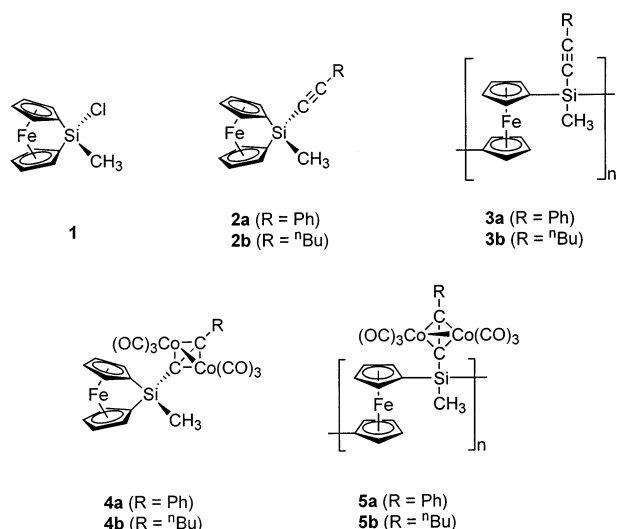
(6) (a) Steffen, W.; Köhler, B.; Altmann, M.; Scherf, U.; Stitzer, K.; zur Loye, H.-C.; Bunz, U. H. F. *Chem. Eur. J.* **2001**, *7*, 117–126. (b) Oriol, L.; Serrano, J. L. *Adv. Mater.* **1995**, *7*, 348–369. (c) Hagihara, N.; Sonogashira, K.; Takahashi, S. *Adv. Polym. Sci.* **1981**, *41*, 149–179.

(7) (a) MacLachlan, M. J.; Ginzburg, M.; Coombs, N.; Coyle, T. W.; Raju, N. P.; Greedan, J. E.; Ozin, G. A.; Manners, I. *Science* **2000**, *287*, 1460–1463. (b) Temple, K.; Kullbaba, K.; Power-Billard, K. N.; Manners, I.; Leach, K. A.; Xu, T.; Russell, T. P.; Hawker, C. J. *Adv. Mater.* **2003**, *15*, 297–300.

(8) (a) Park, C.; McAlvin, J. E.; Fraser, C. L.; Thomas, E. L. *Chem. Mater.* **2002**, *14*, 1225–1230. (b) Massey, J. A.; Winnik, M. A.; Manners, I.; Chan, V. Z.-H.; Ostermann, J. M.; Enchelmaier, R.; Spatz, J. P.; Möller, M. *J. Am. Chem. Soc.* **2001**, *123*, 3147–3148.

possibilities, but in general, this area is very poorly developed. In recent intriguing work, Johnson and co-workers have briefly reported the formation of a highly metallized polymer based on the hexanuclear ruthenium carbido species $\text{Ru}_6\text{C}(\text{CO})_{15}$; this material is electron-beam sensitive and can be used to fabricate ruthenium-based nanoparticle chains and conducting wires.¹⁰ In addition, Humphrey and co-workers have successfully developed a polycondensation approach to yield well-characterized polyurethanes containing tetrahedral Mo_2Ir_2 clusters in the backbone with potentially interesting nonlinear optical properties.¹¹

Ring-opening polymerization (ROP) of strained metallocenophanes is a versatile methodology for the synthesis of high molecular weight polymetalloenes that exhibit a range of interesting characteristics.^{12,13} With the aim of incorporating a higher concentration of metals into these polymers, we have recently found that sila[1]ferrocenophanes **2** with potentially ligating acetylenic substituents are readily accessible via the reaction of sila[1]ferrocenophane **1** with an appropriate lithium acetylide.¹⁴ ROP of species such as **2** yields polyferrocenylsilanes **3** with acetylide side groups.¹⁴ In a recent communication,¹⁵ we have briefly reported that the pendent acetylide substituents in both monomer **2a** and polymer **3a** can be transformed into tetrahedral Co_2C_2 clusters on treatment with dicobalt octacarbonyl to afford species **4a** and **5a**, respectively. We have also shown that polymer **5a** provides a route to ceramics containing magnetic Co/Fe alloy nanoparticles in high yield.¹⁵ In this paper we report full details of our studies on the incorporation of additional metallo fragments via complexation of the triple bond in acetylide-substituted sila[1]ferrocenophanes. In future papers we will provide details on the ROP behavior of these species and the properties and applications of analogous high polymers.



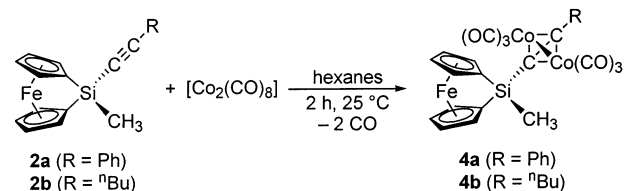
Results and Discussion

Silicon-bridged [1]ferrocenophanes with pendent metallo substituents are rare and at present are limited to

(9) (a) Shriver, D. F.; Kaesz, H. D.; Adams, R. D. *The Chemistry of Metal Cluster Complexes*; VCH Publishers Inc.: New York, 1990. (b) Braunstein, P.; Oro, L. A.; Raithby, P. R., Eds. *Metal Clusters in Chemistry*; VCH Publishers Inc.: New York, 1999.

(10) Johnson, B. F. G.; Sanderson, K. M.; Shephard, D. S.; Ozkaya, D.; Zhou, W.; Ahmed, H.; Thomas, M. D. R.; Gladden, L.; Mantle, M. *Chem. Commun.* **2000**, 1317–1318.

Scheme 1. Reaction of **2a** and **2b** with $[\text{Co}_2(\text{CO})_8]$ and Synthesis of **4a** and **4b**



species with ferrocenyl¹⁶ or $[\text{Co}(\text{CO})_4]$ ¹⁷ groups. To provide a general route to such highly metallized species, we explored complexation to sila[1]ferrocenophanes with one or two acetylenic side groups.

Synthesis and Characterization of Sila[1]ferrocenophanes with a Pendent Organocobalt Cluster (4a and 4b). Reaction of acetylide-substituted sila[1]ferrocenophanes **2a** and **2b** with a slight excess of dicobalt octacarbonyl, $[\text{Co}_2(\text{CO})_8]$, in hexanes led to selective clusterization of the triple bond with a dicobalt hexacarbonyl fragment (Scheme 1). Importantly, ring-opening of the sila[1]ferrocenophane was not observed, in contrast to the situation for a tin-bridged analogue¹⁸ or a sila[1]ferrocenophane containing a silicon–hydrogen bond.¹⁷ After workup and recrystallization from hexanes at $-55\text{ }^\circ\text{C}$, we isolated cobalt-clusterized sila[1]ferrocenophanes **4a** and **4b** as red-purple solids in yields of 65% and 80%, respectively.

The ^1H NMR spectrum of **4a** showed three resonances for phenyl protons at $\delta = 7.72$ (*ortho*), 7.02 (*meta*), and

(11) (a) Lucas, N. T.; Humphrey, M. G.; Rae, A. D. *Macromolecules* **2001**, *34*, 6188–6195. (b) For some other work on cluster polymers, see: Kuhnert, T.; Stradiotto, M.; Ruffolo, R.; Ulbrich, D.; McGlinchey, M. J.; Brook, M. A. *Organometallics* **1997**, *16*, 5048–5057.

(12) (a) Foucher, D. A.; Tang, B.-Z.; Manners, I. *J. Am. Chem. Soc.* **1992**, *114*, 6246–6248. (b) Foucher, D. A.; Honeyman, C. H.; Nelson, J. M.; Tang, B.-Z.; Manners, I. *Angew. Chem., Int. Ed. Engl.* **1993**, *32*, 1709–1711. (c) Rulkens, R.; Gates, D. P.; Balaishis, D.; Pudelski, J. K.; McIntosh, D. F.; Lough, A. J.; Manners, I. *J. Am. Chem. Soc.* **1997**, *119*, 10976–10986. (d) Resendes, R.; Nelson, J. M.; Fischer, A.; Jäkle, F.; Bartole, A.; Lough, A. J.; Manners, I. *J. Am. Chem. Soc.* **2001**, *123*, 2116–2126. (e) Kulbaba, K.; Manners, I. *Macromol. Rapid Commun.* **2001**, *22*, 711–724.

(13) For work by other groups, see: (a) Sharma, H. K.; Cervantes-Lee, F.; Mahmoud, J. S.; Pannell, K. H. *Organometallics* **1999**, *18*, 399–403. (b) Mizuta, T.; Imamura, Y.; Miyoshi, K. *J. Am. Chem. Soc.* **2003**, *125*, 2068–2069. (c) Herberhold, M.; Hertel, F.; Milius, W.; Wrackmeyer, B. *J. Organomet. Chem.* **1999**, *582*, 352–357. (d) Calleja, G.; Carré, F.; Cerveau, G.; Labbé, P.; Coche-Guérente, L. *Organometallics* **2001**, *20*, 4211–4215. (e) Mizuta, T.; Onishi, M.; Miyoshi, K. *Organometallics* **2000**, *19*, 5005–5009. (f) Reddy, N. P.; Yamashita, H.; Tanaka, M. *J. Chem. Soc., Chem. Commun.* **1995**, 2263–2264. (g) Bucaille, A.; Le Borgne, T.; Ephritikhine, M.; Daran, J.-C. *Organometallics* **2000**, *19*, 4912–4914. (h) Osborne, A. G.; Whiteley, R. H. *J. Organomet. Chem.* **1975**, *101*, C27–28. (i) Espada, L. I.; Shadaram, M.; Robillard, J.; Pannell, K. H. *J. Inorg. Organomet. Polym.* **2000**, *10*, 169–176. (j) Broussier, R.; Da Rold, A.; Gautheron, B.; Dromzee, Y.; Jeannin, Y. *Inorg. Chem.* **1990**, *29*, 1817–1822. (k) Papkov, V. S.; Gerasimov, M. V.; Dubovik, I. I.; Sharma, S.; Dementiev, V. V.; Pannell, K. H. *Macromolecules* **2000**, *33*, 7107–7115. (l) Sun, Q.; Xu, K.; Peng, H.; Zheng, R.; Häussler, M.; Tang, B.-Z. *Macromolecules* **2003**, *36*, 2309–2320.

(14) Berenbaum, A.; Lough, A. J.; Manners, I. *Organometallics* **2002**, *21*, 4415–4424.

(15) Berenbaum, A.; Ginzburg-Margau, M.; Coombs, N.; Lough, A. J.; Safa-Sefat, A.; Gredan, J. E.; Ozin, G. A.; Manners, I. *Adv. Mater.* **2003**, *15*, 51–55.

(16) (a) MacLachlan, M. J.; Zheng, J.; Thieme, K.; Lough, A. J.; Manners, I.; Mordas, C.; LeSuer, R.; Geiger, W. E.; Liable-Sands, L. M.; Rheingold, A. L. *Polyhedron* **2000**, *19*, 275–289. (b) Pannell, K. H.; Dementiev, V. V.; Li, H.; Cervantes-Lee, F.; Nguyen, M. T.; Diaz, A. F. *Organometallics* **1994**, *13*, 3644–3650, and references therein.

(17) Berenbaum, A.; Jäkle, F.; Lough, A. J.; Manners, I. *Organometallics* **2001**, *20*, 834–843.

(18) Berenbaum, A.; Jäkle, F.; Lough, A. J.; Manners, I. *Organometallics* **2002**, *21*, 2359–2361.

Table 1. Selected Bond Lengths (Å) and Bond Angles (deg) for 4a

Si(1)–C(1)	1.889(4)	C(12)–Co(2)	1.981(4)	C(11)–Si(1)–C(12)	111.70(18)
Si(1)–C(6)	1.892(4)	C(13)–Co(1)	1.971(4)	Si(1)–C(12)–C(13)	145.7(3)
Si(1)–C(12)	1.841(4)	C(13)–Co(2)	1.971(4)	C(12)–C(13)–C(14)	142.9(3)
C(12)–C(13)	1.334(5)	Co(1)–Co(2)	2.4850(8)	Co(1)–C(13)–Co(2)	78.16(13)
C(13)–C(14)	1.471(5)	Fe(1)–Si(1)	2.6913(11)	Co(2)–C(12)–Co(1)	78.07(13)
C(12)–Co(1)	1.964(4)	C(1)–Si(1)–C(6)	96.52(16)	α	19.09(21)

Table 2. Selected Bond Lengths (Å) and Bond Angles (deg) for 4b

Si(1)–C(1)	1.878(4)	C(12)–Co(2)	1.992(4)	C(11)–Si(1)–C(12)	111.04(17)
Si(1)–C(6)	1.885(4)	C(13)–Co(1)	1.969(4)	Si(1)–C(12)–C(13)	150.5(3)
Si(1)–C(12)	1.832(4)	C(13)–Co(2)	1.975(4)	C(12)–C(13)–C(14)	141.5(4)
C(12)–C(13)	1.340(5)	Co(1)–Co(2)	2.4859(8)	Co(1)–C(13)–Co(2)	78.16(13)
C(13)–C(14)	1.491(5)	Fe(1)–Si(1)	2.6804(12)	Co(2)–C(12)–Co(1)	78.14(15)
C(12)–Co(1)	1.975(4)	C(1)–Si(1)–C(6)	97.11(18)	α	19.51(19)

6.96 (*para*) ppm, all significantly shifted downfield from those of **2a** ($\delta = 7.50$ – 7.47 (*ortho*), 6.95 – 6.92 (*meta* and *para*) ppm).¹⁴ The methyl proton resonance also displayed a similar downfield shift (**4a**: $\delta = 0.73$ ppm; **2a**: $\delta = 0.61$ ppm).¹⁴ Downfield shifts of such magnitude are common to the highly metallized sila[1]ferrocenophanes in this work. We observed four resonances at $\delta = 4.36$, 4.34 , 4.25 , and 3.93 ppm for cyclopentadienyl (Cp) protons; this pattern is characteristic of an unsymmetrically substituted sila[1]ferrocenophane. The $^{13}\text{C}\{^1\text{H}\}$ NMR spectrum of **4a** showed one broad carbonyl resonance at $\delta = 200.1$ ppm, likely due to spin–spin coupling with the quadrupolar cobalt nuclei ($I = 7/2$ for ^{59}Co).¹⁹ Using CIGAR-HMBC spectroscopy,²⁰ a resonance at $\delta = 107.1$ ppm was assigned to the acetylenic carbon bound to the phenyl group and a resonance at $\delta = 74.6$ ppm was assigned to the acetylenic carbon bound to silicon (cf. **2a**: $\delta = 107.7$ and 89.7 ppm for C_{Ph} and C_{Si} , respectively).¹⁴ The *ipso*-Cp carbons of **4a** resonated at $\delta = 33.6$ ppm, downfield from those of **2a** ($\delta = 30.4$ ppm).¹⁴ The $^{29}\text{Si}\{^1\text{H}\}$ NMR spectrum of **4a** showed a singlet at $\delta = -11.8$ ppm, again shifted downfield from that of **2a** ($\delta = -27.8$ ppm).¹⁴ The four carbonyl stretches in the infrared spectrum of **4a** at 2091 , 2055 , 2030 , and 2013 cm^{-1} suggested all carbonyl ligands are terminal.

The ^1H NMR spectrum of **4b** is again consistent with selective clusterization of the hexyne moiety, as resonances for protons of the *n*-butyl chain in **4b** are shifted downfield from those in **2b**. The $^{13}\text{C}\{^1\text{H}\}$ NMR spectrum of **4b** showed a broad carbonyl resonance at $\delta = 200.6$ ppm. The *ipso*-Cp carbons of **4b** resonated at $\delta = 34.2$ ppm, slightly downfield to those of **4a** ($\delta = 33.6$ ppm). The $^{29}\text{Si}\{^1\text{H}\}$ NMR spectrum for **4b** contained a singlet at $\delta = -12.5$ ppm, significantly shifted downfield from that of **2b** ($\delta = -29.1$ ppm).¹⁴ As with **4a**, the infrared spectrum of **4b** showed only terminal carbonyl stretches, at 2089 , 2051 , and 2021 cm^{-1} .

To confirm the assigned structures and compare structural details, single-crystal X-ray diffraction studies were performed for **4a** and **4b**. Figure 1 shows the two molecular structures; Tables 1 and 2 list selected bond lengths and bond angles.

The molecular structures of **4a** and **4b** confirmed the expected atom connectivity. The tilt angles between the Cp rings (α) in **4a** and **4b** were $19.09(21)^\circ$ and $19.51(19)^\circ$, respectively; these are slightly smaller than

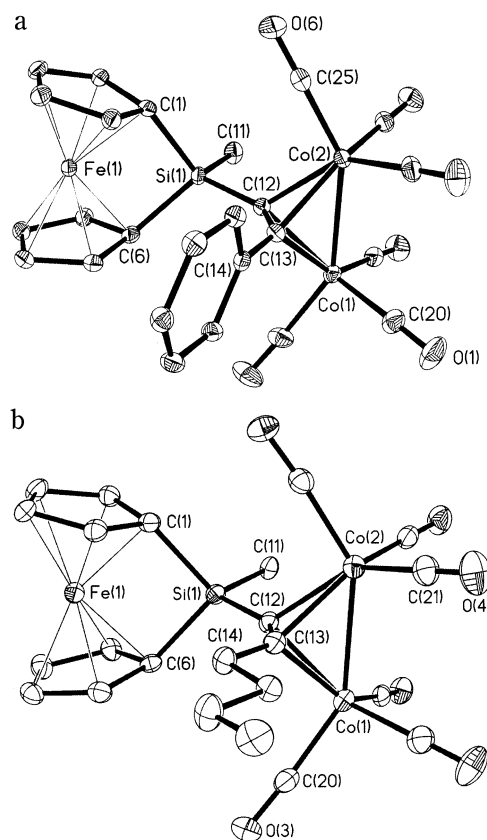


Figure 1. (a) Molecular structure of **4a**. (b) Molecular structure of **4b**. For both structures, thermal ellipsoids are displayed at 30% probability and hydrogen atoms have been omitted for clarity.

that of unclusterized sila[1]ferrocenophane **2a** ($\alpha = 20.53(14)^\circ$).¹⁴ The Fe–Si distances in **4a** ($2.6913(11)$ Å) and **4b** ($2.6804(12)$ Å) fall within the normal range for sila[1]ferrocenophanes (cf. $d(\text{Fe}–\text{Si}) = 2.55$ – 2.75 Å).^{21,22} As found in other $[\text{Co}_2(\text{CO})_6\text{C}_2\text{R}_2]$ clusters, the Co–Co axis in **4a** and **4b** is perpendicular to that of the alkyne.²³ Upon cobalt coordination, the geometry of the alkyne moiety changed from linear to bent. The Si(1)–C(12)–C(13) angles in **4a** and **4b** were $145.7(3)^\circ$ and $150.5(3)^\circ$, respectively, and the C(12)–C(13)–C(14)

(21) Pudelski, J. K.; Foucher, D. A.; Honeyman, C. H.; Lough, A. J.; Manners, I.; Barlow, S.; O'Hare, D. *Organometallics* **1995**, *14*, 2470–2479.

(22) Zechel, D. L.; Hultsch, K. C.; Rulkens, R.; Balaishis, D.; Ni, Y.; Pudelski, J. K.; Lough, A. J.; Manners, I.; Foucher, D. A. *Organometallics* **1996**, *15*, 1972–1978.

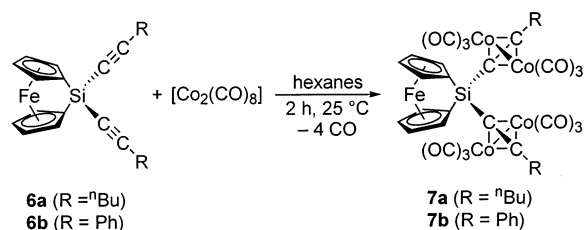
(23) Gregson, D.; Howard, J. A. K. *Acta Crystallogr.* **1983**, *C39*, 1024–1027.

(19) Aime, S.; Milone, L.; Rossetti, R.; Stanghellini, P. L. *Inorg. Chim. Acta* **1977**, *22*, 135–139.

(20) Hadden, C. E.; Martin, G. E.; Krishnamurthy, V. V. *Magn. Reson. Chem.* **2000**, *38*, 143–147.

Table 3. Selected Bond Lengths (Å) and Bond Angles (deg) for 7a

Si(1)–C(1)	1.887(3)	Co(2)–C(18)	1.962(3)	C(17)–Si(1)–C(29)	114.72(13)
Si(1)–C(6)	1.887(3)	Co(3)–C(30)	1.961(3)	Si(1)–C(17)–C(18)	144.4(2)
Si(1)–C(17)	1.859(3)	Co(1)–C(17)	2.004(3)	Si(1)–C(29)–C(30)	148.6(2)
Si(1)–C(29)	1.844(3)	Co(4)–C(29)	2.003(3)	C(17)–C(18)–C(19)	148.2(3)
C(17)–C(18)	1.333(4)	Co(2)–C(17)	1.997(3)	C(29)–C(30)–C(31)	143.3(3)
C(29)–C(30)	1.345(4)	Co(3)–C(29)	2.009(3)	Co(1)–C(18)–Co(2)	78.03(11)
C(18)–C(19)	1.502(4)	Co(1)–Co(2)	2.4811(6)	Co(3)–C(30)–Co(4)	77.78(11)
C(30)–C(31)	1.495(4)	Co(3)–Co(4)	2.4649(6)	Co(1)–C(17)–Co(2)	76.65(10)
Co(1)–C(18)	1.979(3)	Fe(1)–Si(1)	2.6913(9)	Co(3)–C(29)–Co(4)	75.81(11)
Co(4)–C(30)	1.965(3)	C(1)–Si(1)–C(6)	96.52(13)	α	19.87(22)

Scheme 2. Reaction of 6a and 6b with [Co₂(CO)₈] and Synthesis of 7a and 7b

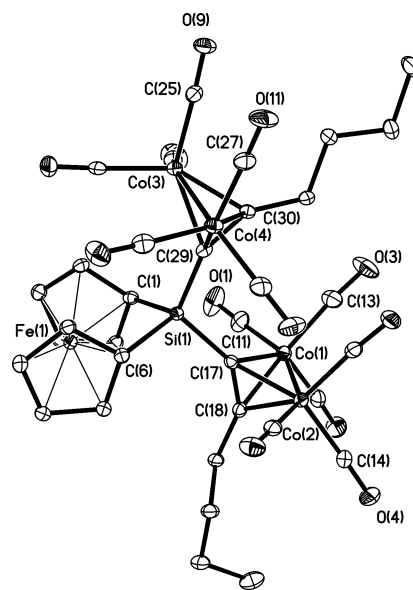
angles were 142.9(3)° and 141.5(4)°. The Co(1)–Co(2) distances in **4a** (2.4850(8) Å) and **4b** (2.4859(8) Å) are typical for clusters of disubstituted alkynes ($d(\text{Co}–\text{Co}) = 2.460–2.477$ Å).²³

Synthesis and Characterization of a Sila[1]-ferrocenophane Containing Two Cobalt Clusters (7a). To increase the metal content of sila[1]ferrocenophanes still further, we explored the analogous complexation of the novel bis(acetylide) monomer **6a**. In a synthesis similar to that of **4a** and **4b**, we reacted **6a** with excess [Co₂(CO)₈] in hexanes to form **7a** (Scheme 2). We found that it was important to use an excess of the cobalt reagent, as the use of a stoichiometric amount gave a mixture of products with either one or two clusterized alkyne moieties. After workup and recrystallization from hexanes at –35 °C, we isolated **7a** as a dark brown solid (yield = 63%).

The ¹H NMR spectrum of **7a** showed two resonances for the α - and β -Cp protons at $\delta = 4.54$ and 4.51 ppm, respectively (cf. **6a**: $\delta = 4.48$ and 4.42 ppm); this pattern is characteristic of a symmetrically substituted sila[1]-ferrocenophane. We observed four resonances at $\delta = 3.15$, 1.84, 1.35, and 0.89 ppm for the four different types of protons on the *n*-butyl chains, shifted downfield from those of **6a** ($\delta = 2.01$, 1.29, and 0.73 ppm). The ¹³C{¹H} and ²⁹Si{¹H} NMR spectra of **7a** are similar to those of **4b** and are consistent with the assigned structure. The infrared spectrum of **7a** contained three terminal carbonyl stretches, at 2084, 2056, and 2026 cm⁻¹.

To confirm the assigned structure, we performed a single-crystal X-ray diffraction study for **7a**. Figure 2 shows the molecular structure of **7a**, and Table 3 lists selected bond lengths and bond angles.

The molecular structure of **7a** was as expected. The tilt angle (19.87(22)°) and Fe–Si distance (2.6913(9) Å) in **7a** were very similar to those in the sila[1]ferrocenophane containing one cobalt-clusterized hexynyl substituent (cf. **4b**: $\alpha = 19.51(19)^\circ$, $d(\text{Fe}–\text{Si}) = 2.6804(12)$ Å). Both hexynyl moieties in **7a** exhibited a bent geometry, with bond angles around the alkyne carbons ranging from ca. 143° to 149°. The Co(1)–Co(2) and Co(3)–Co(4) distances were 2.4811(6) and

**Figure 2.** Molecular structure of **7a** (thermal ellipsoids at 30% probability). Hydrogen atoms have been removed for clarity.

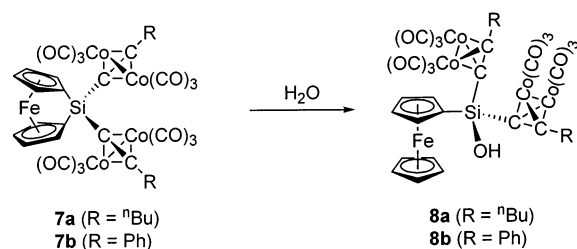
2.4649(6) Å, respectively; the slight asymmetry of the two clusters is probably a result of crystal-packing forces.

Isolation of an Unexpected Side Product; Hydrolytic Ring-Opening of 7b to Form a Silanol (8b). When a benzene solution of **7a** was left at 25 °C, new resonances appeared in the ¹H NMR spectrum after 1 day. Among the new signals, the singlet at $\delta = 4.05$ ppm is characteristic for a C₅H₅ moiety and suggests ring-opening of the sila[1]ferrocenophane to afford **8a**.²⁴ When we prepared **7b** (the phenylacetylide analogue of **7a**) from **6b** and [Co₂(CO)₈], we found that this conversion was even more facile. Over a three-week recrystallization, the desired product **7b** quantitatively converted to the corresponding ring-opened product **8b** (Scheme 3), which was fully characterized. The ¹H NMR spectrum of **8b** contained a singlet at $\delta = 4.05$ ppm for protons of the free Cp ligand, whereas protons of the other Cp ligand resonated at $\delta = 4.57$ and 4.24 ppm. A singlet at $\delta = 2.84$ ppm was assigned to a silanol –OH group. The ¹³C{¹H} NMR spectrum of **8b** contained a broad carbonyl resonance at $\delta = 200.0$ ppm. We observed five Cp carbon resonances between $\delta = 74.7$ and 69.1 ppm, in contrast to two for sila[1]ferrocenophane **7a**. The ²⁹Si{¹H} NMR spectrum of **8b** contained a singlet at $\delta = -13.4$ ppm. In the IR spectrum of **8b**, four terminal carbonyl stretches were found at 2087, 2054, 2026, and 2009 cm⁻¹.

(24) Fischer, A. B.; Kinney, J. B.; Staley, R. H.; Wrighton, M. S. *J. Am. Chem. Soc.* **1979**, *101*, 6501–6506.

Table 4. Selected Bond Lengths (Å) and Bond Angles (deg) for 8b

Si(1)–C(1)	1.845(2)	Co(1)–C(12)	1.959(3)	C(25)–C(26)–C(33)	140.3(2)
Si(1)–C(11)	1.843(3)	Co(3)–C(26)	1.969(2)	Co(1)–C(11)–Co(2)	75.74(9)
Si(1)–C(25)	1.840(2)	Co(2)–C(12)	1.978(2)	Co(3)–C(25)–Co(4)	75.88(8)
C(11)–C(12)	1.340(3)	Co(4)–C(26)	1.981(2)	Co(1)–C(12)–Co(2)	77.49(9)
C(25)–C(26)	1.346(3)	Co(1)–Co(2)	2.4637(5)	Co(3)–C(26)–Co(4)	76.99(8)
C(12)–C(19)	1.459(3)	Co(3)–Co(4)	2.4588(4)	C(1)–Si(1)–C(11)	108.07(11)
C(26)–C(33)	1.463(3)	Si(1)–O(13)	1.656(2)	C(1)–Si(1)–C(25)	113.72(11)
Co(1)–C(11)	1.992(2)	C(11)–Si(1)–C(25)	109.59(11)	C(1)–Si(1)–O(13)	110.14(11)
Co(3)–C(25)	2.002(2)	Si(1)–C(11)–C(12)	150.3(2)	C(11)–Si(1)–C(25)	109.59(11)
Co(2)–C(11)	2.021(2)	Si(1)–C(25)–C(26)	149.45(19)	C(11)–Si(1)–O(13)	105.94(11)
Co(4)–C(25)	1.997(2)	C(11)–C(12)–C(19)	143.6(2)	C(25)–Si(1)–O(13)	109.08(11)

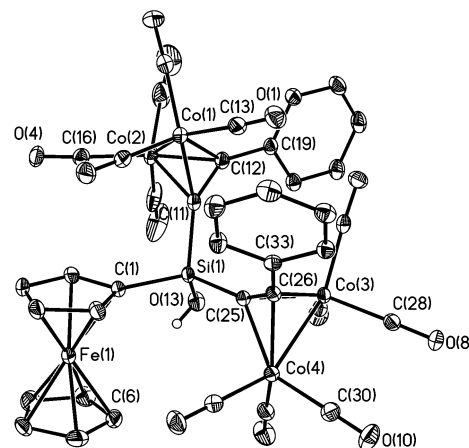
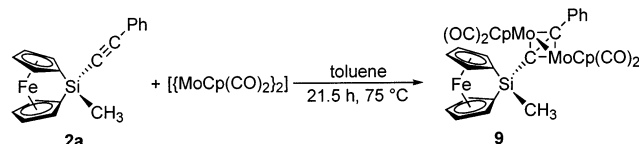
Scheme 3. Ring-Opening of 7a and 7b to Form Silanols 8a and 8b

To further confirm the structure of the ring-opened product, we performed a single-crystal X-ray diffraction study for **8b**. Figure 3 shows the molecular structure of **8b**, and Table 4 lists selected bond lengths and bond angles.

The molecular structure of **8b** shows two intact cobalt clusters, in agreement with the assigned structure. The ring-opening reaction had little effect on the structure of the cobalt clusters, as the cobalt–cobalt and acetylenic bond lengths showed minimal changes. The silicon atom of **8b** displayed a distorted tetrahedral geometry, with bond angles around silicon ranging from ca. 106° to 114°. The presence of two bulky cobalt-clusterized phenylacetylene substituents led to a larger than ideal C(1)–Si(1)–C(25) angle (113.72(11)°) and a smaller than ideal C(11)–Si(1)–O(13) angle (105.94(11)°). No intermolecular hydrogen bonding is apparent, presumably due to the steric bulk around silicon. The lack of hydrogen bonding is in contrast to the situation for many other ferrocenyl silanol species.^{16a,25}

Synthesis and Characterization of a Sila[1]-ferrocenophane with Pendent Organomolybdenum Clusters (9). To expand the clusterization chemistry to other metals, we explored complexation of the acetylide group of **2a** using an organomolybdenum reagent. Overnight heating of a toluene solution of **2a** and $[\{\text{MoCp}(\text{CO})_2\}_2]$ at 75 °C resulted in addition of a dimolybdenum unit to the triple bond of the phenylacetylene substituent (Scheme 4). After workup and recrystallization from a mixture of hexanes and dichloromethane at –35 °C, we isolated **9** as a dark red-purple solid (yield = 38%). The same clusterization through decarbonylation of $[\{\text{MoCp}(\text{CO})_3\}_2]$ proved sluggish, with less than 10% conversion after 21 h at 85 °C in tetrahydrofuran.

The ¹H NMR spectrum of **9** contained phenyl resonances at δ = 7.67 (*ortho*), 7.18–7.12 (*meta*), and 6.92

**Figure 3.** Molecular structure of **8b** (thermal ellipsoids at 30% probability). Hydrogen atoms have been removed for clarity.**Scheme 4. Reaction of 2a with $[\{\text{MoCp}(\text{CO})_2\}_2]$ and Synthesis of 9**

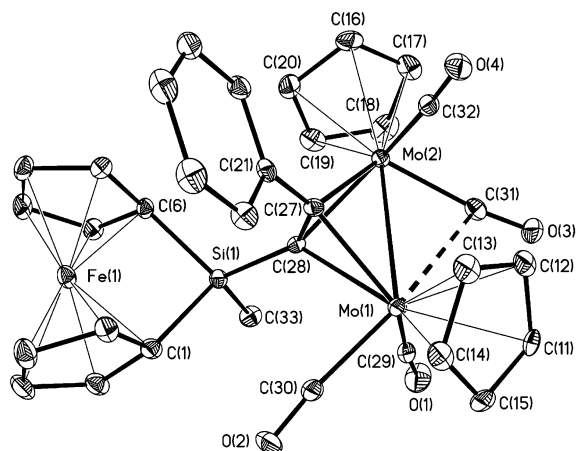
(*para*) ppm, downfield to those of **2a**.¹⁴ Upon coordination, the resonance for protons of the Cp rings bound to molybdenum shifted downfield from δ = 4.62 to 4.99 ppm. The ¹³C{¹H} NMR spectrum of **9** contained two resonances in the carbonyl region: a broad signal at δ ≈ 233 ppm and a sharp signal at δ = 230.5 ppm. However, we would expect four carbonyl resonances when $[\{\text{MoCp}(\text{CO})_2\}_2]$ coordinates to an unsymmetrical alkyne to form a Mo₂C₂ core. On the basis of a previous variable-temperature NMR study of $[\text{Cp}_2\text{Mo}_2(\text{CO})_4(\text{RC}\equiv\text{CR}')]_2$ complexes,²⁶ this observation can be explained by the simultaneous occurrence of a low-energy and a higher-energy process. The low-energy process interconverts the two molybdenum atoms, the two Cp ligands, and the two pairs of carbonyl ligands; the higher-energy process allows partial rotation of the Mo–Mo bond. As a result, only two types of carbonyl ligands are observed at 25 °C. The presence of a single molybdenum Cp resonance at δ = 92.2 ppm also supports this explanation. Upon coordination to molybdenum, the resonance for *ipso*-Cp carbons shifted downfield from δ = 30.4 to 37.8 ppm. We observed a singlet at δ = –3.8 ppm in the ²⁹Si{¹H} NMR spectrum of **9**, significantly shifted downfield from that of **2a** (δ = –27.8 ppm).¹⁴

(25) For some recent work on ferrocenyl silanols, see: (a) MacLachlan, M. J.; Zheng, J.; Lough, A. J.; Manners, I.; Mordas, C.; LeSuer, R.; Geiger, W. E.; Liable-Sands, L. M.; Rheingold, A. L. *Organometallics* **1999**, *18*, 1337–1345. (b) Reyes-Garcia, E. A.; Cervantes-Lee, F.; Pannell, K. H. *Organometallics* **2001**, *20*, 4734–4740.

(26) Bailey, W. I., Jr.; Chisholm, M. H.; Cotton, F. A.; Rankel, L. A. *J. Am. Chem. Soc.* **1978**, *100*, 5764–5773.

Table 5. Selected Bond Lengths (Å) and Bond Angles (deg) for 9

Si(1)–C(1)	1.894(4)	Mo(2)–C(27)	2.200(3)	C(28)–Si(1)–C(33)	113.16(17)
Si(1)–C(6)	1.899(3)	Mo(1)–C(28)	2.240(3)	C(27)–C(28)–Si(1)	142.2(3)
Si(1)–C(28)	1.841(4)	Mo(2)–C(28)	2.170(3)	C(21)–C(27)–C(28)	136.4(3)
C(27)–C(28)	1.366(5)	Mo(1)–Mo(2)	2.9625(4)	Mo(1)–C(27)–Mo(2)	85.11(12)
C(21)–C(27)	1.482(5)	Fe(1)–Si(1)	2.7202(11)	Mo(1)–C(28)–Mo(2)	84.40(12)
Mo(1)–C(27)	2.181(3)	C(1)–Si(1)–C(6)	95.18(16)	α	20.93(20)

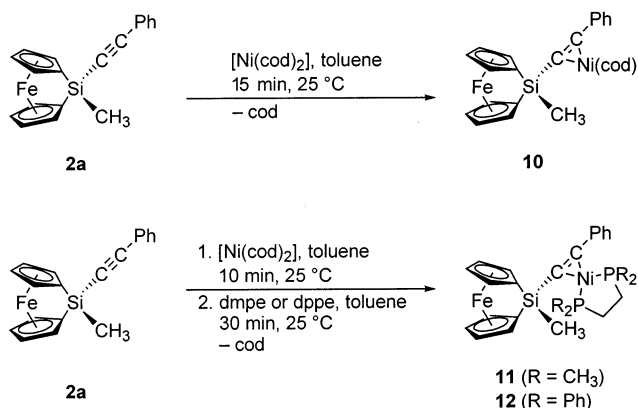
**Figure 4.** Molecular structure of **9** (thermal ellipsoids at 30% probability). Hydrogen atoms have been removed for clarity.

The infrared spectrum of **9** showed three stretches at 1988, 1923, and 1837 cm^{-1} , suggesting both terminal and semibridging carbonyl ligands are present.²⁷

To confirm the assigned structure, we performed a single-crystal X-ray diffraction study for **9**. Figure 4 shows the molecular structure of **9**, and Table 5 lists selected bond lengths and bond angles.

The X-ray study confirmed the identity of **9**. The tilt angle (20.93(20)°) and Fe–Si distance (2.7202(11) Å) in **9** are typical for sila[1]ferrocenophanes. Although the tilt angle remained virtually unchanged (cf. **2a**: $\alpha = 20.53(14)^\circ$) upon molybdenum coordination, the C(1)–Si(1)–C(6) angle decreased from 96.50(13)° to 95.18(6)°. Also, the Mo–Mo distance increased from 2.448(1) to 2.9625(4) Å, in agreement with other compounds containing a Mo₂C₂ core. For example, the analogous diphenylacetylene and diethylacetylene complexes have Mo–Mo distances of 2.965(1) and 2.977(1) Å, respectively.²⁶ Bonding between the alkyne and the dimolybdenum unit can be described by the Dewar–Chatt–Duncanson model:^{28,29} Acetylenic carbons became sp³-like upon molybdenum coordination, with both substituents bending back from the C–C bond axis. The acetylenic C–C bond length increased significantly from 1.197(4) to 1.366(5) Å, slightly longer than that of free ethylene ($d(\text{C}=\text{C}) = 1.34$ Å).³⁰ The C(27)–C(28)–Si(1) angle was 142.2(3)°, and the C(21)–C(27)–C(28) angle was 136.4(3)°. As observed in previously characterized [Cp₂Mo₂(CO)₄(RC≡CR')] complexes,²⁶ **9** also contains a semibridging carbonyl ligand (see Figure 4).

Synthesis and Characterization of Sila[1]ferrocenophanes with a Pendent Organonickel Complex (11 and 12). We also attempted to expand the

Scheme 5. Top: Reaction of 2a with [Ni(cod)₂] to Form 10. Bottom: Reaction of 2a with [Ni(cod)₂] and dmpe or dppe and Synthesis of 11 and 12

clusterization chemistry to nickel via complexation of the alkyne substituent in **2a**.³¹ When **2a** was reacted with bis(1,5-cyclooctadiene)nickel(0), [Ni(cod)₂], in toluene, the methyl and phenyl resonances of **2a** and the olefinic resonances of cyclooctadienyl ligand shifted downfield. This observation is consistent with the addition of a nickel moiety to the triple bond of the phenylacetylene substituent of **2a** to form **10** (Scheme 5, top). However, all attempts to separate the desired product from unidentified side products were unsuccessful, possibly due to subsequent dissociation of the labile cod ligand. We postulated that replacement of the cod ligand with a stronger donor, such as a bidentate bisphosphine, should result in stabilization of the complex. After the reaction of **2a** with [Ni(cod)₂], 1,2-bis(dimethylphosphino)ethane (dmpe) or 1,2-bis(diphenylphosphino)ethane (dppe) was added; this led to substitution of the cod ligand with dmpe or dppe and the formation of **11** or **12**, respectively (Scheme 5, bottom). After workup and recrystallization from a mixture of toluene and hexanes at –35 °C, we obtained **11** as a red-orange solid (yield = 61%). We isolated **12** as an orange solid after workup (yield = 56%).

The ¹H NMR spectrum of **11** contained three resonances for phenyl protons at $\delta = 8.13$ (*ortho*), 7.28 (*meta*), and 7.10 (*para*) ppm and four resonances for Cp protons at $\delta = 4.47$, 4.38, 4.29, and 4.15 ppm. A doublet of triplets at $\delta = 1.22$ ppm was assigned to the four methyl groups of dmpe. The four methylene protons were found as a doublet at $\delta = 1.13$ ppm. The ¹³C{¹H} NMR spectrum of **11** contained two resonances for acetylenic carbons at $\delta = 159.1$ and 158.8 ppm, extremely deshielded compared to those of **2a** ($\delta = 107.7$ and 89.7 ppm).¹⁴ Nevertheless, downfield shifts of 40 to 55 ppm have been reported in the literature for [Ni(dippe)(RC≡CR)] complexes (dippe = bis(diisopropyl-

(27) Le Berre-Cosquer, B.; Kergoat, R.; L'Haridon, P. *Organometallics* **1992**, *11*, 721–728.

(28) Dewar, M. J. S. *Bull. Soc. Chim. Fr.* **1951**, C71–79.

(29) Chatt, J.; Duncanson, L. A. *J. Chem. Soc.* **1953**, 2939–2947.

(30) Elschenbroich, C.; Salzer, A. *Organometallics: A Concise Introduction*; VCH Publishers Inc.: New York, 1992.

(31) We also attempted to complex the alkyne substituent using [Fe₂(CO)₉]. However, ¹H NMR (C₆D₆) analysis of the reaction mixture in tetrahydrofuran (2 h, 25 °C) indicated a complex mixture of products. This clusterization was not further pursued.

Table 6. Selected Bond Lengths (Å) and Bond Angles (deg) for 11

Si(1)–C(1)	1.887(2)	Ni(1)–P(1)	2.1602(7)	C(12)–Ni(1)–C(13)	39.84(10)
Si(1)–C(6)	1.888(2)	Ni(1)–P(2)	2.1462(7)	P(2)–Ni(1)–C(13)	116.53(7)
Si(1)–C(12)	1.811(2)	Fe(1)–Si(1)	2.7013(7)	P(1)–Ni(1)–P(2)	90.13(3)
C(12)–C(13)	1.288(3)	C(1)–Si(1)–C(6)	96.07(10)	P(1)–Ni(1)–C(12)	113.66(8)
C(13)–C(14)	1.457(3)	C(11)–Si(1)–C(12)	113.97(12)	α	19.90(13)
Ni(1)–C(12)	1.905(2)	Si(1)–C(12)–C(13)	154.67(19)		
Ni(1)–C(13)	1.875(2)	C(12)–C(13)–C(14)	143.0(2)		

Table 7. Selected Bond Lengths (Å) and Bond Angles (deg) for 12

Si(1)–C(1)	1.897(3)	Ni(1)–P(1)	2.1434(7)	C(11)–Ni(1)–C(12)	39.60(10)
Si(1)–C(6)	1.889(2)	Ni(1)–P(2)	2.1605(7)	P(1)–Ni(1)–C(12)	116.81(8)
Si(1)–C(11)	1.823(3)	Fe(1)–Si(1)	2.7209(7)	P(1)–Ni(1)–P(2)	89.67(3)
C(11)–C(12)	1.284(3)	C(1)–Si(1)–C(6)	95.13(10)	P(2)–Ni(1)–C(11)	113.68(8)
C(12)–C(13)	1.461(3)	C(11)–Si(1)–C(19)	110.61(2)	α	20.38(10)
Ni(1)–C(11)	1.904(2)	Si(1)–C(11)–C(12)	153.9(2)		
Ni(1)–C(12)	1.887(2)	C(11)–C(12)–C(13)	141.5(2)		

phosphino)ethane).³² The *ipso*-phenyl carbon of **11** resonated at $\delta = 135.7$ ppm, downfield to that of **2a** ($\delta = 123.0$ ppm). The five resonances between $\delta = 125$ – 132 ppm were assigned to the remaining phenyl carbons and toluene molecules in the crystal lattice. The resonance for *ipso*-Cp carbons at $\delta = 37.6$ ppm was also significantly shifted downfield from that of **2a** ($\delta = 30.4$ ppm).¹⁴ All of the carbons in the dmpe ligand coupled to the phosphorus atoms: Methyl carbons gave four doublets between $\delta = 30.3$ and 29.8 ppm, and methylene carbons gave two doublets of doublets at $\delta = 16.6$ and 16.0 ppm. Unlike ^1H resonances, ^{13}C resonances indicate the two ends of the dmpe ligand are inequivalent. The $^{29}\text{Si}\{^1\text{H}\}$ NMR spectrum of **11** contained a doublet of doublets at $\delta = 23.2$ ppm, a result of coupling to two inequivalent phosphorus atoms ($^3J_{\text{SiP}} = 16.5$ and 11.9 Hz). The two strongly coupled resonances at $\delta = 22.44$ and 22.40 ppm in the $^{31}\text{P}\{^1\text{H}\}$ NMR spectrum of **11** support the assignment of two inequivalent phosphorus atoms.

The ^1H and $^{13}\text{C}\{^1\text{H}\}$ NMR spectra of **12** are similar to those for **11**, except P–Ph resonances are present instead of P–Me signals. The methyl proton resonance of **12** at $\delta = 0.39$ ppm is unusual in that it is shifted upfield from that of **2a** ($\delta = 0.61$ ppm), whereas all other highly metallized sila[1]ferrocenophanes described in this work exhibit downfield shifts.¹⁴ The *ipso*-Cp carbons of **12** resonated at $\delta = 36.7$ ppm ($^4J_{\text{CP}} = 3.8$ Hz), slightly downfield to those of **2a** ($\delta = 30.4$ ppm).¹⁴ The $^{29}\text{Si}\{^1\text{H}\}$ NMR spectrum of **12** showed a doublet of doublets at $\delta = 22.3$ ppm ($^3J_{\text{SiP}} = 17.8, 8.7$ Hz), indicative of coupling to two inequivalent phosphorus atoms. The $^{31}\text{P}\{^1\text{H}\}$ NMR spectrum of **12** contained two doublets at $\delta = 52.9$ and 51.7 ppm ($^2J_{\text{PP}} = 61$ Hz).

We performed single-crystal X-ray diffraction studies for **11** and **12** to confirm the assigned structures. Figure 5 shows the molecular structures of **11** and **12**; Tables 6 and 7 list selected bond lengths and bond angles. The X-ray studies confirmed the proposed structures of **11** and **12**. The tilt angles in **11** ($19.90(13)^\circ$) and **12** ($20.38(10)^\circ$) were slightly smaller than that of **2a** ($\alpha = 20.53(14)^\circ$).¹⁴ The C(1)–Si(1)–C(6) angles were $96.07(10)^\circ$ in **11** and $95.13(10)^\circ$ in **12**, and the corresponding Fe(1)–Si(1) distances were $2.7013(7)$ and $2.7209(7)$ Å, respectively. These parameters are similar to those of **9**. In both **11** and **12**, the nickel atom had a

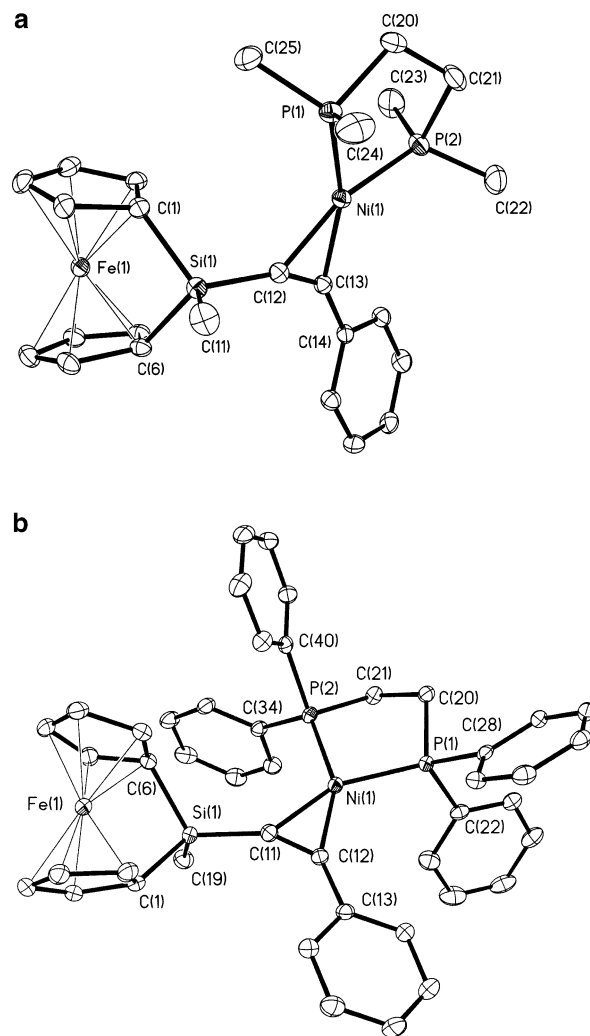


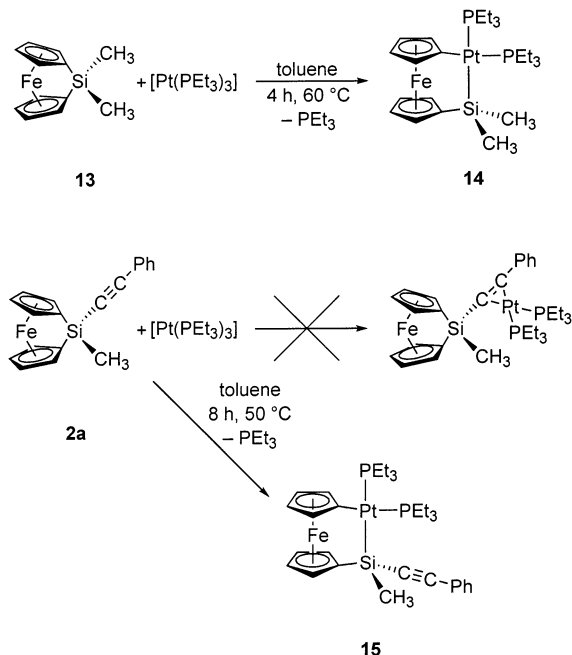
Figure 5. (a) Molecular structure of **11**. (b) Molecular structure of **12**. For both structures, thermal ellipsoids are displayed at 30% probability and hydrogen atoms have been removed for clarity.

distorted square-planar geometry. Although the angles around nickel summed to 360° (**11**: 360.16° ; **12**: 359.76°), the C–Ni–C angle was much more acute than the remaining angles. Nickel–carbon bond lengths in **11** and **12** ranged from 1.875 to 1.905 Å, similar to those in $[\text{Ni}(\text{dmpe})(\text{PhC}\equiv\text{CPh})]$ ($d(\text{Ni}–\text{C}) = 1.876$ – 1.879 Å).³³

(32) Edelbach, B. L.; Lachicotte, R. J.; Jones, W. D. *Organometallics* **1999**, *18*, 4040–4049.

(33) Pörschke, K. R.; Mynott, R.; Angermund, K.; Krüger, C. Z. *Naturforsch.* **1985**, *40b*, 199–209.

Scheme 6. Insertion of Pt(PEt₃)₂ into Sila[1]ferrocenophanes **13 and **2a** to Form Platinasila[2]ferrocenophanes **14** and **15****



Acetylenic C–C bond lengths were 1.288(3) and 1.284(3) Å in **11** and **12**, respectively, approaching that of free ethylene ($d(\text{C}=\text{C}) = 1.34$ Å).³⁰ To the best of our knowledge, **11** and **12** are the first examples of stable mononuclear nickel alkyne complexes derived from [Ni(cod)₂] and an alkyne, as previous work has shown that [Ni(cod)₂] reacts with dialkyl- and diarylacetylenes to form a dinuclear cluster, [Ni₂(cod)₂(RC≡CR)].³⁴ Examination of the molecular structures of **11** and **12** indicated that addition of a second nickel moiety to the alkyne would probably be sterically disfavored. Therefore, even when we reacted **2a** with excess [Ni(cod)₂], only the mononuclear nickel complex was formed.

Reaction of Acetylide-Substituted Sila[1]ferrocenophane **2a with Tris(triethylphosphine)platinum(0): Insertion of a Platinum(0) Fragment into an *ipso*-Cp Carbon–Silicon Bond to form a [2]-Ferrocenophane (**15**).** Finally, to expand the clusterization chemistry still further, we explored the possibility of adding platinum(0) units via complexation of the alkyne substituent in **2a**. This is complicated by the tendency of platinum(0) fragments to undergo oxidative insertion into an *ipso*-Cp carbon–silicon bond of sila[1]ferrocenophanes: Previous work has shown that [Pt(PEt₃)₃] reacts with sila[1]ferrocenophane **13** to give the platinasila[2]ferrocenophane **14** (Scheme 6, top).^{35,36} Nevertheless, we wanted to explore if the reactivity of [Pt(PEt₃)₃] would be changed by the presence of a coordinating alkyne substituent. When a toluene solution of [Pt(PEt₃)₃] and **2a** was stirred at 50 °C for 8 h, only platinasila[2]ferrocenophane **15** was formed (Scheme

(34) Muetterties, E. L.; Pretzer, W. R.; Thomas, M. G.; Beier, B. F.; Thorn, D. L.; Day, V. W.; Anderson, A. B. *J. Am. Chem. Soc.* **1978**, *100*, 2090–2096.

(35) Sheridan, J. B.; Temple, K.; Lough, A. J.; Manners, I. *J. Chem. Soc., Dalton Trans.* **1997**, 711–713.

(36) (a) Sheridan, J. B.; Lough, A. J.; Manners, I. *Organometallics* **1996**, *15*, 2195–2197. (b) Reddy, N. P.; Choi, N.; Shimada, S.; Tanaka, M. *Chem. Lett.* **1996**, 649–650.

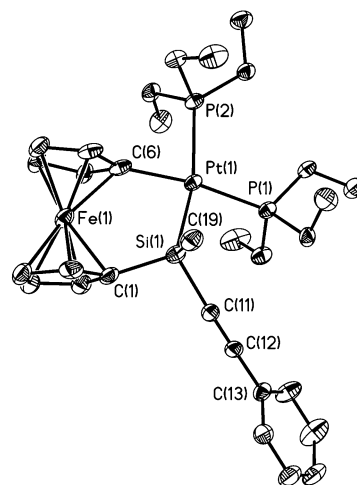


Figure 6. Molecular structure of **15** (thermal ellipsoids at 30% probability). Hydrogen atoms have been removed for clarity.

6, bottom). After workup, we isolated red-orange crystals of **15** by slowly evaporating a dichloromethane/hexanes solution at 25 °C (yield = 55%).

We used ¹H, ¹³C, ²⁹Si, ³¹P NMR, COSY, HSQC, and CIGAR-HMBC²⁰ spectroscopy to confirm the assigned structure for **15**, since the 1-D spectra were complex due to the large number of NMR-active nuclei. The ¹H NMR spectrum of **15** clearly indicates loss of the strained sila[1]ferrocenophane structure. We observed eight resonances for Cp protons between $\delta = 5.01$ and 4.11 ppm, indicating that the two Cp rings are inequivalent. The two multiplets at $\delta = 2.20$ –2.08 and 1.99–1.89 ppm were assigned to diastereotopic methylene protons of the phosphine ligand *cis* to the chiral silicon atom. Methylene protons of the phosphine ligand *trans* to the silicon atom were found at $\delta = 1.26$ ppm as a doublet of quartets; these protons coupled to a phosphorus atom (²J_{HP} = 7.2 Hz) and three neighboring methyl protons (³J_{HH} = 7.2 Hz) with the same coupling constant. A doublet at $\delta = 1.12$ ppm was assigned to the methyl group bound to silicon; it showed coupling to phosphorus (⁴J_{HP} = 2.1 Hz) and platinum satellites (³J_{HPt} = 13.9 Hz). The ¹³C{¹H} NMR spectrum of **15** contained 10 resonances for Cp carbons between $\delta = 80.7$ and 69.0 ppm. The *ipso*-Cp carbon bound to silicon resonated at $\delta = 80.7$ ppm, and the corresponding carbon bound to platinum appeared as a doublet of doublets at $\delta = 71.6$ ppm (²J_{CP} = 99.9 and 13.3 Hz). These resonances shifted significantly downfield from that of the *ipso*-Cp carbons in **2a** ($\delta = 30.4$ ppm),¹⁴ a result of the release of ring strain in forming a [2]ferrocenophane. In the ²⁹Si{¹H} NMR spectrum of **15**, a doublet of doublets with platinum satellites at $\delta = -16.9$ ppm (¹J_{SiPt} = 1433 Hz, ²J_{SiP} = 208.8 and 18.3 Hz) indicated coupling of silicon to the two phosphorus atoms. The ³¹P{¹H} NMR spectrum of **15** contained two doublets with platinum satellites at $\delta = 12.2$ (¹J_{Pt} = 1137 Hz, ²J_{PP} = 20.0 Hz) and 11.7 ppm (¹J_{Pt} = 2132 Hz, ²J_{PP} = 20.0 Hz), showing coupling between the two inequivalent phosphorus atoms. To confirm the assigned structure of **15**, we performed a single-crystal X-ray diffraction study. Figure 6 shows the molecular structure of **15**, and Table 8 lists selected bond lengths and bond angles.

Table 8. Selected Bond Lengths (Å) and Bond Angles (deg) for 15

Si(1)–C(1)	1.871(9)	C(1)–Si(1)–C(11)	102.4(4)	P(2)–Pt(1)–C(6)	83.3(2)
Si(1)–Pt(1)	2.378(2)	C(1)–Si(1)–C(19)	105.8(4)	Si(1)–C(11)–C(12)	177.8(8)
Pt(1)–C(6)	2.068(9)	C(1)–Si(1)–Pt(1)	116.5(3)	C(11)–C(12)–C(13)	178.2(9)
Pt(1)–P(1)	2.291(2)	C(6)–Pt(1)–Si(1)	82.2(2)	α	9.36(64)
Pt(1)–P(2)	2.395(2)	Si(1)–Pt(1)–P(1)	92.60(8)	β_{Si}	16.1(4)
Si(1)–C(11)	1.874(9)	P(1)–Pt(1)–P(2)	103.39(8)	β_{Pt}	6.5(3)

The X-ray study confirmed the assigned structure of **15**. The tilt angle of 9.36(64)° in **15** suggests it is less strained than **14** ($\alpha = 11.6(3)^\circ$).³⁶ The angle between the plane of the top Cp ring and the *ipso*-Cp carbon–platinum bond (β) was 6.5(3)°, and the β angle between the plane of the bottom Cp ring and the *ipso*-Cp carbon–silicon bond was 16.1(4)°. A difference in β angles was also observed in **14**.³⁶ The platinum atom in **15** had a distorted square-planar geometry, with a larger than ideal P(1)–Pt(1)–P(2) angle (103.39(8)°) and smaller than ideal Si(1)–Pt(1)–C(6) and P(2)–Pt(1)–C(6) angles (82.2(2)° and 83.3(2)°, respectively). The two platinum–phosphorus bonds in **15** had almost the same length ($d(\text{Pt}–\text{P}) = 2.291(2), 2.395(2)$ Å), similar to those in **14** ($d(\text{Pt}–\text{P}) = 2.2931(13), 2.4060(13)$ Å).³⁶

Summary

We have described the synthesis of highly metallized sila[1]ferrocenophanes containing cobalt, molybdenum, or nickel units via direct reaction of an acetylide-substituted sila[1]ferrocenophane with an appropriate organometallic precursor.³¹ The nature of the product depended on the metal: Cobalt and molybdenum gave dinuclear clusters, while nickel gave mononuclear complexes. The total number of metal clusters was also controlled by varying the number of acetylenic substituents in the sila[1]ferrocenophane.

The highly metallized sila[1]ferrocenophanes described in this work displayed interesting structural features and reactivity. Species **11** and **12** are the first examples of stable mononuclear nickel complexes formed from a disubstituted alkyne and [Ni(cod)₂]: The usual tendency to form a dinuclear cluster is presumably greatly diminished due to steric crowding around the alkyne. In the presence of trace amounts of moisture, sila[1]ferrocenophanes **7a** and **7b** readily ring-opened in solution to form silanols with intact cobalt clusters. The synthesis of a sila[1]ferrocenophane with a pendent organoplatinum unit remains a challenge, as the reaction of **2a** with [Pt(PEt₃)₃] yielded only a platinasila[2]-ferrocenophane.

We are currently exploring the ROP behavior of these highly metallized sila[1]ferrocenophanes as well as the properties and applications of the resulting polymers. The results of these detailed studies will be subjects of future publications.¹⁵

Experimental Section

[Ni(cod)₂], dmpe, and dppe were purchased from Aldrich and used as received. [Co₂(CO)₈] and [MoCp(CO)₃]₂ were purchased from STREM; [Co₂(CO)₈] was sublimed immediately before use. Reactions involving [Co₂(CO)₈] require ambient light to proceed. Compounds **2a**,¹⁴ **2b**,¹⁴ **6b**,¹⁴ [MoCp(CO)₂]₂,³⁷ and [Pt(PEt₃)₄]³⁸ were synthesized according to literature procedures.

(37) Ginley, D. S.; Bock, C. R.; Wrighton, M. S. *Inorg. Chim. Acta* **1997**, *23*, 85–94.

All manipulations were performed under an atmosphere of prepurified nitrogen using Schlenk techniques or in an inert atmosphere glovebox. Solvents were dried using the Grubbs method³⁹ or standard methods followed by distillation. ¹H (300 MHz), ¹³C (75.5 MHz), and ³¹P (121.5 MHz) NMR spectra were recorded on a Varian Gemini 300 or Mercury 300 spectrometer. ¹H (400 MHz), ¹³C (100.5 MHz), and ²⁹Si (79.4 MHz) NMR spectra were recorded on a Varian Unity 400 spectrometer. ¹H (500 MHz), ¹³C (125.6 MHz), and 2-D NMR spectra were recorded on a Varian Inova 500 spectrometer. ¹H resonances were referenced internally to the residual protonated solvent resonances. ¹³C resonances were referenced internally to the deuterated solvent resonances. ²⁹Si and ³¹P resonances were referenced externally to TMS and H₃PO₄ resonances, respectively. Mass spectra were recorded with a VG 70-250S mass spectrometer in electron impact (EI) mode. The calculated isotopic distribution for each ion was in agreement with experimental values. Infrared spectra were recorded using a Perkin-Elmer Spectrum One FT-IR spectrometer. Ultraviolet–visible spectra were recorded using a Perkin-Elmer Lambda 900 UV/VIS/NIR spectrometer. Elemental analyses were performed using a Perkin-Elmer 2400 C/H/N analyzer.

Synthesis of 4a. [Co₂(CO)₈] (0.86 g, 2.5 mmol) in hexanes (150 mL) was added dropwise to a stirred solution of **2a** (0.75 g, 2.3 mmol) in hexanes (300 mL). The reaction mixture was stirred at 25 °C for 2 h while vented through an oil bubbler to release evolved CO. The flask was cooled to –55 °C, and **4a** precipitated as a red-purple microcrystalline solid, yield 0.92 g (65%). Crystals suitable for X-ray diffraction studies were obtained from a dichloromethane/hexanes (1:1 v/v) solution at –30 °C.

For **4a**: ¹H NMR (400 MHz, C₆D₆, 25 °C) $\delta = 7.72$ (d, ³J_{HH} = 7.2 Hz, 2 H, *ortho*-Ph), 7.02 (t, ³J_{HH} = 7.2 Hz, 2 H, *meta*-Ph), 6.96 (d, ³J_{HH} = 7.2 Hz, 1 H, *para*-Ph), 4.36 (m, 2 H, Cp), 4.34 (m, 2 H, Cp), 4.25 (m, 2 H, Cp), 3.93 (m, 2 H, Cp) 0.73 (s, 3 H, Me); ¹³C{¹H} NMR (100.5 MHz, C₆D₆, 25 °C) δ 200.1 (CO), 138.6 (*ipso*-Ph), 130.1, 129.3, 128.4 (Ph), 107.1 (SiCCPh), 78.6, 78.2, 76.0, 75.9 (Cp), 74.6 (SiCCPh), 33.6, (*ipso*-Cp), –1.9 (Me); ²⁹Si{¹H} NMR (79.4 MHz, C₆D₆, 25 °C) $\delta = -11.8$; MS (70 eV, EI) *m/z* (%) 656 (24) [(2 × fcSiMe(CCPH))⁺], 614 (2) [M]⁺, 328 (100) [fcSiMe(CCPH)]⁺, 286 (10) [(Co₂(CO)₆]⁺, 186 (26) [fc]⁺; HRMS (70 eV, EI) calcd for C₂₅H₁₆Co₂⁵⁶FeO₆Si 613.872952, found 613.873412, fit 0.7 ppm; FT-IR (25 °C, hexanes) $\nu(\text{CO})$ 2091 (m), 2055 (s), 2030 (s), 2013 (w) cm⁻¹; UV–vis (25 °C, THF) $\lambda_{\text{max}} = 443$ nm, $\epsilon = 2.2 \times 10^3$ L·mol⁻¹·cm⁻¹, abs > 0 until ca. 700 nm.}}}

Synthesis of 4b. [Co₂(CO)₈] (1.15 g, 3.4 mmol) in hexanes (200 mL) was added to a stirred solution of **2b** (1.04 g, 3.4 mmol) in hexanes (100 mL). The reaction mixture was stirred at 25 °C for 1 h while vented through an oil bubbler to release evolved CO, and all volatile materials were removed in vacuo. The residue was taken up in hexanes and filtered through glass wool to remove small amounts of insoluble impurities. Dark red-purple crystals of **4b** were obtained at –55 °C, yield 1.61 g (80%). Crystals suitable for X-ray diffraction studies were obtained from a hexanes solution at –30 °C.

For **4b**: ¹H NMR (400 MHz, C₆D₆, 25 °C) δ 4.46 (m, 2 H, Cp), 4.37 (m, 2 H, Cp), 4.23 (m, 2 H, Cp), 3.92 (m, 2 H, Cp), 2.96 (m, 2 H, CH₂CH₂CH₂CH₃), 1.76 (m, 2 H, CH₂CH₂CH₂–

(38) Yoshida, T.; Matsuda, T.; Otsuka, S. *Inorg. Synth.* **1990**, *28*, 122–123.

(39) Pangborn, A. B.; Giardello, M. A.; Grubbs, R. H.; Rosen, R. K.; Timmers, F. J. *Organometallics* **1996**, *15*, 1518–1520.

CH₃), 1.28 (m, 2 H, CH₂CH₂CH₂CH₃), 0.84 (t, 3 H, ³J_{HH} = 7.2 Hz, CH₂CH₂CH₂CH₃), 0.72 (s, 3 H, SiCH₃); ¹³C{¹H} NMR (100.5 MHz, C₆D₆, 25 °C) δ 200.6 (CO), 113.1 (SiCPh), 72.5 (SiCCPh) 78.4, 78.1, 75.8, 75.7 (Cp), 34.9 (CH₂CH₂CH₂CH₃), 34.8 (CH₂CH₂CH₂CH₃), 34.2 (*ipso*-Cp), 22.9 (CH₂CH₂CH₂CH₃), 13.9 (CH₂CH₂CH₂CH₃), -2.7 (SiCH₃); ²⁹Si{¹H} NMR (79.4 MHz, C₆D₆, 25 °C) δ -12.5; MS (70 eV, EI) *m/z* (%) 594 (34) [M]⁺, 538 (62) [M - 2 CO]⁺, 510 (53) [M - 3 CO]⁺, 482 (69) [M - 4 CO]⁺, 308 (100) [M - Co₂(CO)₆]⁺; HRMS (70 eV, EI) calcd for C₂₃H₂₀Co₂⁵⁶FeO₆Si 593.904252, found 593.902933, fit 2.2 ppm; FT-IR (25 °C, hexanes) ν(CO) 2089 (m), 2051 (s), 2021 (s) cm⁻¹. Anal. Calcd for C₂₃H₂₀Co₂FeO₆Si: C 46.49, H 3.39. Found: C 46.24, H 3.29.

Synthesis of 6a. This compound was synthesized using a procedure analogous to that for the phenylacetylide-substituted analogue (**6b**).¹⁴ Yield: 83% (crude, >95% pure).

For 6a: ¹H NMR (500 MHz, C₆D₆, 25 °C) δ 4.48 (m, 4 H, Cp), 4.42 (m, 4 H, Cp), 2.01 (t, ³J_{HH} = 7.0 Hz, 4 H, CH₂CH₂-CH₂CH₃), 1.29 (m, 8 H, CH₂CH₂CH₂CH₃), 0.73 (t, ³J_{HH} = 7.0 Hz, 6 H, CH₃); ¹³C{¹H} NMR (100.5 MHz, C₆D₆, 25 °C) δ 110.5 (SiCCBu), 78.28(Cp), 78.24 (SiCCBu), 30.4 (CH₂CH₂CH₂CH₃), 29.6 (*ipso*-Cp), 22.1 (CH₂CH₂CH₂CH₃), 19.8 (CH₂CH₂CH₂CH₃), 13.6 (CH₃); ²⁹Si{¹H} NMR (79.4 MHz, C₆D₆, 25 °C) δ -56.0; MS (70 eV, EI) *m/z* (%) 374 (100) [M]⁺; HRMS (70 eV, EI) calcd for C₂₂H₂₆⁵⁶FeSi 374.115319, found 374.115293, fit 0.1 ppm.

Synthesis of 7a. [Co₂(CO)₈] (413 mg, 1.2 mmol) in hexanes (5 mL) was added portionwise to a stirred solution of **6a** (152 mg, 0.41 mmol) in hexanes (5 mL). The reaction mixture was stirred at 25 °C for 1 h while vented through an oil bubbler to release evolved CO. All volatile materials were removed in vacuo to give a dark brown solid. Recrystallization from hexanes at -35 °C gave dark brown crystals from which a small amount of [Co₄(CO)₁₂] was removed by sublimation, yield 243 mg, 63%. Crystals suitable for X-ray diffraction studies were obtained from the same sublimation.

For 7a: ¹H NMR (500 MHz, C₆D₆, 25 °C) δ 4.54 (m, 4 H, Cp), 4.51 (m, 4 H, Cp), 3.15 (t, ³J_{HH} = 8.5 Hz, 4 H, CH₂CH₂-CH₂CH₃), 1.84 (pentet, ³J_{HH} = 8.0 Hz, 4 H, CH₂CH₂CH₂CH₃), 1.35 (sextet, ³J_{HH} = 7.0 Hz, 4 H, CH₂CH₂CH₂CH₃), 0.89 (t, ³J_{HH} = 7.5 Hz, 6 H, CH₃); ¹³C{¹H} NMR (75.5 MHz, C₆D₆, 25 °C) δ 200.7 (CO), 115.1 (SiCCBu), 78.9, 76.5 (Cp), 70.2 (SiCCBu), 35.7 (CH₂CH₂CH₂CH₃), 35.0 (CH₂CH₂CH₂CH₃), 34.6 (*ipso*-Cp), 23.1 (CH₂CH₂CH₂CH₃), 14.1 (CH₃); ²⁹Si{¹H} NMR (79.4 MHz, C₆D₆, 25 °C) δ -18.4; MS analysis was not possible as the sample decomposed in the spectrometer; also, the molecular weight of this compound is too high for HRMS; FT-IR (25 °C, hexanes) ν(CO) 2084 (m), 2056 (s), 2026 (s, contains a shoulder) cm⁻¹. Anal. Calcd for C₃₄H₂₆Co₄FeO₁₂Si: C 43.16, H 2.77. Found: C 35.65, H 2.68. We attribute the low carbon value to the presence of a trace amount of [Co₄(CO)₁₂]. A band corresponding to [Co₄(CO)₁₂] was observed in the infrared spectrum at 1867 cm⁻¹; the intensity of this band is about 3% of that at 2026 cm⁻¹ ([Co₄(CO)₁₂] shows two CO stretches at 1900 and 1867 cm⁻¹ in the bridging region, see ref 40). Despite subliming the sample at room temperature for 2 days, we were unable to completely remove [Co₄(CO)₁₂]. We were also unable to separate [Co₄(CO)₁₂] from **7a** by recrystallization, as both compounds are soluble in hexanes.

Formation of 8a from the Hydrolytic Ring-Opening of 7a. A deuterated benzene solution of crude **7a** showed new ¹H resonances after standing 1 day at 25 °C (ca. 30% conversion). The new resonances have chemical shifts very similar to those of **8b**. By analogy, the new compound was assigned as **8a**.

For 8a (only partial data are given, as the solution contained a mixture of **7a** and **8a**, making it difficult to obtain accurate integral values.): ¹H NMR (500 MHz, C₆D₆, 25 °C) δ 4.38 (m, Cp), 4.21 (m, Cp), 4.05 (s, free Cp), 3.01 (m, CH₂CH₂CH₂CH₃),

2.49 (s, SiOH), 1.75 (m, CH₂CH₂CH₂CH₃), 1.34 (m, CH₂CH₂CH₂-CH₃), 0.89 (m, CH₃).

Attempted Synthesis of 7b; Unexpected Formation of 8b. [Co₂(CO)₈] (253 mg, 0.74 mmol) in hexanes (10 mL) was added dropwise to a stirred solution of **6b** (100 mg, 0.24 mmol) in hexanes (10 mL). The solution was stirred at 25 °C for 2 h while vented to an oil bubbler to release evolved CO. All volatile material was removed in vacuo to give a dark brown residue. This was dissolved in ether, and the solution was allowed to evaporate at 25 °C. Silanol **8b** was formed as the sole product after three weeks. Crystals suitable for X-ray diffraction studies were obtained from a hexanes/CH₂Cl₂ (3:1 v/v) solution at -35 °C.

For 7b: ¹H NMR (400 MHz, C₆D₆, 25 °C) δ 7.63–7.60 (m, 4 H, *ortho*-Ph), 6.92–6.89 (m, 6 H, *meta*-, *para*-Ph), 4.59 (m, 4 H, Cp), 4.42 (m, 4 H, Cp); ¹³C{¹H} NMR (100.5 MHz, C₆D₆, 25 °C) δ 200.3 (CO), 138.7 (*ipso*-Ph), 130.7, 129.1 (Ph), 78.8, 76.3 (Cp), 34.0 (*ipso*-Cp).

For 8b: ¹H NMR (400 MHz, C₆D₆, 25 °C) δ 7.75 (d, ³J_{HH} = 7.6 Hz, 4 H, *ortho*-Ph), 7.06 (dd, ³J_{HH} = 7.6, 7.6 Hz, 4 H, *meta*-Ph), 6.96 (dd, ³J_{HH} = 7.6, 7.6 Hz, 2 H, *para*-Ph), 4.57 (m, 2 H, Cp), 4.24 (m, 2 H, Cp), 4.05 (s, 5 H, free Cp), 2.84 (s, 1 H, SiOH); ¹³C{¹H} NMR (100.5 MHz, C₆D₆, 25 °C) δ 200.0 (CO), 138.2, 130.5, 129.2, 128.6 (Ph), 106.5 (SiCPh), 74.7, 72.6, 71.8, 69.6, 69.1 (Cp); ²⁹Si{¹H} NMR (79.4 MHz, C₆D₆, 25 °C) δ -13.4; MS analysis was not possible due to the low volatility of **8b**; FT-IR (25 °C, hexanes) ν(CO) 2087 (m), 2054 (s), 2026 (s), 2009 (w) cm⁻¹. Anal. Calcd for C₃₈H₂₀Co₄FeO₁₃Si: C 45.45, H 2.01. Found: C 45.39, H 1.91.

Synthesis of 9. 2a (204 mg, 0.62 mmol) and [MoCp(CO)₂]₂ (274 mg, 0.63 mmol) were dissolved in toluene (20 mL), and the dark red solution was stirred at 75 °C for 21.5 h. After cooling to 25 °C, all volatile materials were removed in vacuo. The residue was recrystallized from hexanes/dichloromethane (7:6 v/v) at -35 °C to give dark red-purple crystals of **9**, yield 181 mg (38%). Crystals suitable for X-ray diffraction studies were obtained by slow evaporation of an ethereal solution.

For 9: ¹H NMR (300 MHz, C₆D₆, 25 °C) δ 7.67 (d, ³J_{HH} = 7.6 Hz, 2 H, *ortho*-Ph), 7.18–7.12 (m, 2 H, *meta*-Ph), 6.92 (t, ³J_{HH} = 7.6 Hz, 1 H, *para*-Ph), 4.99 (br s, 10 H, Cp_{Mo}), 4.51–4.49 (m, 2 H, Cp_{Fe}), 4.41–4.39 (m, 2 H, Cp_{Fe}), 4.33 (br s, 2 H, Cp_{Fe}), 4.03–4.02 (m, 2 H, Cp_{Fe}), 0.68 (s, 3 H, Me); ¹³C{¹H} NMR (125.6 MHz, C₆D₆, 25 °C) δ 233, 230.5 (CO), 147.9 (*ipso*-Ph), 130.8, 128.3, 126.2 (Ph), 92.2 (Cp_{Mo}), 78.0, 77.6, 76.2, 76.1 (Cp_{Fe}), 37.8 (*ipso*-Cp), -1.7 (Me); ²⁹Si{¹H} DEPT NMR (79.4 MHz, C₆D₆, 25 °C) δ -3.8; MS (70 eV, EI) *m/z* (%) 552 (1) [M - 2Cp - 3CO]⁺, 524 (14) [M - 2Cp - 4CO]⁺, 432 (19) [M - 2Cp - 4CO - Mo]⁺; FT-IR (25 °C, CH₂Cl₂) ν(CO) 1988 (m), 1923 (s), 1837 (w) cm⁻¹. Anal. Calcd for C₃₃H₂₆FeMo₂O₄Si: C 51.99, H 3.44. Found: C 51.54, H 3.46.

Attempted Synthesis of 10. In the absence of light, [Ni(cod)₂] (84 mg, 0.31 mmol) was added to a stirred solution of **2a** (101 mg, 0.31 mmol) in toluene (5 mL). The mixture was stirred at 25 °C for 15 min, and all volatile material was removed in vacuo. Recrystallization from hexane/toluene (4:1 v/v) at -35 °C failed to remove the unidentified side products.

For 10: ¹H NMR (300 MHz, C₆D₆, 25 °C) δ 7.78–7.74 (m, 2 H, *ortho*-Ph), 7.17–7.12 (m, 2 H, *meta*-Ph), 7.08–7.04 (m, 1 H, *para*-Ph), 5.95 (s, 2 H, cod), 5.50 (s, 2 H, cod), 4.44, 4.41, 4.26, 4.08 (m, 8 H, Cp), 2.18–2.02 (m, 4 H, cod), 1.98–1.84 (m, 4H, cod), 0.67 (s, 3 H, Me).

Synthesis of 11. In the absence of light, [Ni(cod)₂] (136 mg, 0.49 mmol) was added to a stirred solution of **2a** (160 mg, 0.49 mmol) in toluene (14 mL). The mixture was stirred at 25 °C for 10 min, and a solution of dmpe (73 mg, 0.49 mmol) in toluene (2 mL) was added. After 30 min, all volatile materials were removed in vacuo to give an orange solid. Recrystallization from toluene/hexanes (2:1 v/v) at -35 °C gave red-orange crystals, yield 175 mg, 61%. Crystals suitable for X-ray diffraction studies were obtained from the same recrystallization.

(40) Darensbourg, D. J.; Incurvia, M. J. *Inorg. Chem.* **1980**, *19*, 2585–2590.

Table 9. Selected Crystal, Data Collection, and Refinement Parameters for **4a**, **4b** and **7a**

	4a	4b	7a
formula	C ₂₅ H ₁₆ Co ₂ FeO ₆ Si	C ₂₃ H ₂₀ Co ₂ FeO ₆ Si	C ₃₄ H ₂₆ Co ₄ FeO ₁₂ Si
<i>M_r</i>	614.18	594.19	946.21
cryst syst	triclinic	monoclinic	triclinic
space group	<i>P</i> 1	<i>P</i> 2 ₁ / <i>c</i>	<i>P</i> 1
<i>a</i> , Å	8.2617(4)	14.3173(4)	11.6454(3)
<i>b</i> , Å	8.3552(17)	11.5858(3)	12.5364(4)
<i>c</i> , Å	18.4860(7)	15.4520(5)	13.7397(5)
α, deg	99.881(3)	90	83.3740(10)
β, deg	100.468(3)	111.1340(10)	75.3260(10)
γ, deg	101.146(2)	90	70.852(2)
<i>V</i> , Å ³	1202.6(3)	2390.74(12)	1831.95(10)
<i>Z</i>	2	4	2
ρ _{calc} , g cm ⁻³	1.696	1.651	1.715
μ(Mo Kα), mm ⁻¹	2.048	2.057	2.253
<i>F</i> (000)	616	1200	948
cryst size, mm ³	0.15 × 0.13 × 0.07	0.24 × 0.10 × 0.06	0.24 × 0.12 × 0.08
θ range, deg	2.56–27.50	2.83–25.01	2.70–27.56
no. of reflns collected	26 617	14 450	25 842
no. of indep reflns	5498 (<i>R</i> _{int} = 0.039)	4201 (<i>R</i> _{int} = 0.081)	8400 (<i>R</i> _{int} = 0.0712)
abs corr	semiempirical from equivalents	semiempirical from equivalents	semiempirical from equivalents
max. and min. transmn coeff	0.8699 and 0.7487	0.8865 and 0.6381	0.678 and 0.614
no. of params refined	328	301	470
GoF on <i>F</i> ²	1.138	0.986	1.001
<i>R</i> 1 ^a (<i>I</i> > 2σ(<i>I</i>))	0.0465	0.0411	0.0397
w <i>R</i> 2 ^b (all data)	0.1094	0.0916	0.0885
peak and hole, e Å ⁻³	0.545 and -0.633	0.384 and -0.364	0.502 and -0.636

$$^a R1 = \sum ||F_o| - |F_c|| / \sum |F_o|. \quad ^b wR2 = \{ \sum [w(F_o^2 - F_c^2)^2] / \sum [w(F_o^2)^2] \}^{1/2}.$$

For **11**: ¹H NMR (300 MHz, C₆D₆, 25 °C) δ 8.13 (d, ³*J*_{HH} = 7.5 Hz, 2 H, *ortho*-Ph), 7.28 (t, ³*J*_{HH} = 7.5 Hz, 2 H, *meta*-Ph), 7.10 (t, ³*J*_{HH} = 7.5 Hz, 1 H, *para*-Ph), 4.47 (m, 2 H, Cp), 4.38 (m, 2 H, Cp), 4.29 (m, 2 H, Cp), 4.15 (m, 2 H, Cp), 1.22 (dt, ²*J*_{HP} = 40.8 Hz, ⁴*J*_{HH} = 3.0 Hz, 12 H, CH₃ of dmpe), 1.13 (d, ²*J*_{HP} = 12.8 Hz, 4 H, CH₂), 0.74 (s, 3 H, SiCH₃); ¹³C{¹H} NMR (100.5 MHz, C₆D₆, 25 °C) δ 159.1, 158.8 (m, SiCCPh), 135.7 (*ipso*-Ph), 131.3 (Ph), 129.3 (toluene in lattice), 128.5 (Ph, toluene in lattice), 126.7 (Ph), 125.6 (toluene in lattice), 77.42, 77.36, 77.2, 75.3 (Cp), 37.6 (*ipso*-Cp), 30.3 (d, ¹*J*_{CP} = 21.3 Hz, CH₃ of dmpe), 30.1 (d, ¹*J*_{CP} = 21.3 Hz, CH₃ of dmpe), 30.0 (d, ¹*J*_{CP} = 21.4 Hz, CH₃ of dmpe), 29.8 (d, ¹*J*_{CP} = 21.4 Hz, CH₃ of dmpe), 21.4 (toluene in lattice), 16.6 (dd, ¹*J*_{CP} = 12.3 Hz, ²*J*_{CP} = 9.1 Hz, CH₂), 16.0 (dd, ¹*J*_{CP} = 13.8 Hz, ²*J*_{CP} = 9.1 Hz, CH₂), -2.1 (SiCH₃); ²⁹Si{¹H} DEPT NMR (79.4 MHz, C₆D₆, 25 °C) δ 23.2 (dd, ³*J*_{SIP} = 16.5, 11.9 Hz); ³¹P{¹H} NMR (121.5 MHz, C₆D₆, 25 °C) δ 22.44, 22.40 (2nd order spectrum); MS analysis was not possible, as the sample decomposed in the spectrometer. Anal. Calcd for C_{28.5}H₃₆FeNiP₂Si: C 58.70, H 6.22. Found: C 58.77, H 6.07.

Synthesis of 12. In the absence of light, **2a** (151 mg, 0.46 mmol) was dissolved in toluene (15 mL) to give a red solution. [Ni(cod)₂] (126 mg, 0.46 mmol) was added, and the red solution darkened within 1 min. It was stirred at 25 °C for 10 min, and dppe (181 mg, 0.46 mmol) was added. After 30 min, all volatile materials were removed in vacuo. The residue was washed twice with hexanes to give an orange solid **12**, yield 203 mg (56%). Crystals suitable for X-ray diffraction studies were obtained from a dichloromethane/hexanes (1:1 v/v) solution at -35 °C.

For **12**: ¹H NMR (400 MHz, C₆D₆, 25 °C) δ 7.95 (d, ³*J*_{HH} = 8.4 Hz, 2 H, *ortho*-Ph), 7.81–7.77 (m, 4 H, Ph and Ph_{dppe}), 7.74–7.68 (m, 4 H, Ph_{dppe}), 7.04–6.92 (m, 15 H, Ph_{dppe}), 4.38 (m, 2 H, Cp), 4.33 (m, 2 H, Cp), 4.31 (m, 2 H, Cp), 3.98 (m, 2 H, Cp), 2.10–1.98 (m, 4 H, CH₂), 0.39 (s, 3 H, Me); ¹³C{¹H} NMR (100.5 MHz, C₆D₆, 25 °C) δ 158.6 (d, ²*J*_{CP} = 6.6 Hz, SiCCPh), 158.2 (d, ²*J*_{CP} = 5.3 Hz, SiCCPh), 136.6 (dd, ¹*J*_{CP} = 27.4 Hz, ³*J*_{CP} = 6.1 Hz, *ipso*-Ph of dppe), 136.3 (dd, ¹*J*_{CP} = 28.2 Hz, ³*J*_{CP} = 6.1 Hz, *ipso*-Ph of dppe), 135.7 (dd, ³*J*_{CP} = 11.5, 5.3 Hz, *ipso*-Ph), 133.8 (d, ²*J*_{CP} = 13.8 Hz, *ortho*-Ph of dppe), 133.3 (d, ²*J*_{CP} = 13.7 Hz, *ortho*-Ph of dppe), 131.2 (d, ⁴*J*_{CP} = 3.8 Hz, *ortho*-Ph), 129.6 (d, ⁴*J*_{CP} = 1.5 Hz, *para*-Ph of dppe), 129.5 (d,

⁴*J*_{CP} = 13.8 Hz, *para*-Ph of dppe), 128.7 (d, ³*J*_{CP} = 9.1 Hz, *meta*-Ph of dppe), 128.5 (d, ³*J*_{CP} = 8.3 Hz, *meta*-Ph of dppe), 128.3, 126.6 (Ph), 77.2 (Cp × 2), 77.0, 75.1 (Cp), 36.7 (d, ⁴*J*_{CP} = 3.8 Hz, *ipso*-Cp), 29.4 (dd, ¹*J*_{CP} = 19.1 Hz, ²*J*_{CP} = 15.3 Hz, CH₂), 29.0 (dd, ¹*J*_{CP} = 19.1 Hz, ²*J*_{CP} = 15.3 Hz, CH₂), -2.9 (SiCH₃); ²⁹Si{¹H} DEPT NMR (79.4 MHz, C₆D₆, 25 °C) δ 22.3 (dd, ³*J*_{SIP} = 17.8, 8.7 Hz); ³¹P{¹H} NMR (121.5 MHz, C₆D₆, 25 °C) δ 52.9 (d, ²*J*_{PP} = 61 Hz), 51.7 (d, ²*J*_{PP} = 61 Hz); MS analysis was not possible, as the sample decomposed in the spectrometer. Anal. Calcd for C₄₅H₄₀FeNiP₂Si: C 68.81, H 5.13. Found: C 69.11, H 5.48.

Synthesis of 15. [Pt(PEt₃)₄] (204 mg, 0.31 mmol) was heated under high vacuum at 60 °C until conversion of the white powder into an orange oil, [Pt(PEt₃)₃], was complete (ca. 30 min). Toluene (25 mL) was added to [Pt(PEt₃)₃], and a solution of **1a** (100 mg, 0.30 mmol) in toluene (15 mL) was added dropwise with stirring. The reaction mixture was stirred at 50 °C for 8 h. All volatile materials were removed in vacuo, and the orange-red solid was taken up in a minimal amount of hexanes/dichloromethane (1:1 v/v). Crystals of **15** were obtained by slow evaporation of this solution, yield 125 mg (55%). Crystals suitable for X-ray crystallography studies were obtained using the same method.

For **15**: ¹H NMR (500 MHz, C₆D₆, 25 °C) δ 7.51–7.48 (m, 2 H, *ortho*-Ph), 7.03–7.00 (m, 2 H, *meta*-Ph), 6.98–6.95 (m, 1 H, *para*-Ph), 5.01, 4.85 (m, 2 H, α-Cp_{Si}), 4.55 (m, 1 H, β-Cp_{Pt}), 4.49 (m, 1 H, β-Cp_{Si}), 4.42 (m, 1 H, β-Cp_{Pt}), 4.29 (m, 1 H, β-Cp_{Si}), 4.16, 4.11 (m, 2 H, α-Cp_{Pt}), 2.20–2.08 (m, 3 H, P(CHHCH₃)₃), 1.99–1.89 (m, 3 H, P(CHHCH₃)₃), 1.26 (dq, ³*J*_{HH} = 7.2 Hz, ²*J*_{HP} = 7.2 Hz, 6 H, P(CH₂CH₃)₃), 1.12 (d, ³*J*_{HPt} = 13.9 Hz, ⁴*J*_{HP} = 2.1 Hz, SiCH₃), 0.97 (dt, ³*J*_{HP} = 15.3 Hz, ³*J*_{HH} = 7.8 Hz, 9 H, P(CHHCH₃)₃), 0.77 (dt, ³*J*_{HP} = 14.7 Hz, ³*J*_{HH} = 7.5 Hz, 9 H, P(CH₂CH₃)₃); ¹³C{¹H} NMR (125.6 MHz, C₆D₆, 25 °C) δ 131.4 (*ortho*-Ph × 2), 128.3 (*meta*-Ph × 2), 127.4 (*para*-Ph), 125.8 (*ipso*-Ph), 107.5 (dd, ²*J*_{CPT} = 88 Hz, ³*J*_{CP} = 18.2, 3.5 Hz, SiCCPh), 106.3 (d, ³*J*_{CPT} = 31 Hz, ⁴*J*_{CP} = 4.7 Hz, SiCCPh), 80.7 (m, *ipso*-Cp_{Si}), 75.9, 75.6 (α-Cp_{Si}), 75.2 (d, ²*J*_{CPT} = 64 Hz, ³*J*_{PC} = 6.0 Hz, α-Cp_{Pt}), 73.5 (dd, ²*J*_{CPT} = 46 Hz, ³*J*_{CP} = 5.0, 3.3 Hz, α-Cp_{Pt}), 71.9 (β-Cp_{Si}), 71.6 (dd, ²*J*_{CP} = 99.9, 13.3 Hz, *ipso*-Cp_{Pt}), 71.5 (d, ³*J*_{CPT} = 52 Hz, ⁴*J*_{CP} = 6.0 Hz, β-Cp_{Pt}), 69.7 (d, ³*J*_{CPT} = 50 Hz, ⁴*J*_{CP} = 5.5 Hz, β-Cp_{Pt}), 69.0 (β-Cp_{Si}), 17.7 (dd, ²*J*_{CPT} = 26 Hz, ¹*J*_{CP} = 28.3 Hz, ³*J*_{CP} = 4.3 Hz, P(CHHCH₃)₃),

Table 10. Selected Crystal, Data Collection, and Refinement Parameters for 8b, 9 and 11

	8b	9	11
formula	C ₃₈ H ₂₀ Co ₄ FeO ₁₃ Si	C ₃₃ H ₂₆ FeMo ₂ O ₄ Si	C ₂₅ H ₃₂ FeNiP ₂ Si·0.5C ₇ H ₈
<i>M_r</i>	1004.20	762.36	583.16
cryst syst	triclinic	triclinic	triclinic
space group	<i>P</i> $\bar{1}$	<i>P</i> $\bar{1}$	<i>P</i> $\bar{1}$
<i>a</i> , Å	10.3489(2)	8.6700(2)	10.6560(2)
<i>b</i> , Å	11.1236(3)	9.9580(2)	12.0500(2)
<i>c</i> , Å	16.7606(4)	18.3510(6)	12.6570(3)
α , deg	85.3030(10)	76.2870(12)	62.6990(8)
β , deg	86.2970(10)	89.0310(12)	87.3300(8)
γ , deg	85.2870(10)	67.6720(13)	77.0250(8)
<i>V</i> , Å ³	1913.19(8)	1419.06(6)	1404.32(5)
<i>Z</i>	2	2	2
ρ_{calc} , g cm ⁻³	1.743	1.784	1.379
$\mu(\text{Mo K}\alpha)$, mm ⁻¹	2.165	1.455	1.359
<i>F</i> (000)	1000	760	610
cryst size, mm ³	0.40 × 0.35 × 0.35	0.20 × 0.06 × 0.03	0.30 × 0.20 × 0.14
θ range, deg	2.60–27.50	2.80–27.50	2.59–27.56
no. of reflns collected	27 530	16 977	20 633
no. of indep reflns	8779 (<i>R</i> _{int} = 0.0407)	6474 (<i>R</i> _{int} = 0.0542)	6446 (<i>R</i> _{int} = 0.0488)
abs corr	semiempirical from equivalents	semiempirical from equivalents	semiempirical from equivalents
max. and min. transmn coeff	0.5178 and 0.4780	0.958 and 0.912	0.831 and 0.767
no. of params refined	518	371	296
GoF on <i>F</i> ²	1.017	1.038	1.079
<i>R</i> 1 ^a (<i>I</i> > 2 σ (<i>I</i>))	0.0343	0.0373	0.0382
w <i>R</i> 2 ^b (all data)	0.0876	0.0869	0.1059
peak and hole, e Å ⁻³	1.792 and -0.717	0.750 and -0.810	0.375 and -0.507

$$^a R1 = \sum ||F_o| - |F_c|| / \sum |F_o|. \quad ^b wR2 = \{ \sum [w(F_o^2 - F_c^2)^2] / \sum [w(F_o^2)^2] \}^{1/2}.$$

Table 11. Selected Crystal, Data Collection, and Refinement Parameters for 12 and 15

	12	15
formula	C ₄₅ H ₁₀ FeNiP ₂ Si	C ₃₁ H ₄₆ FeP ₂ PtSi
<i>M_r</i>	785.36	759.65
cryst syst	triclinic	monoclinic
space group	<i>P</i> $\bar{1}$	<i>P</i> 2 ₁ / <i>n</i>
<i>a</i> , Å	11.5830(3)	10.3650(3)
<i>b</i> , Å	12.0940(3)	20.3410(7)
<i>c</i> , Å	14.8820(4)	15.1410(6)
α , deg	108.2460(11)	90
β , deg	92.8720(12)	90.7320(18)
γ , deg	106.6890(8)	90
<i>V</i> , Å ³	1873.92(8)	3191.98(19)
<i>Z</i>	2	4
ρ_{calc} , g cm ⁻³	1.392	1.581
$\mu(\text{Mo K}\alpha)$, mm ⁻¹	1.039	4.988
<i>F</i> (000)	816	1520
cryst size, mm ³	0.30 × 0.20 × 0.18	0.18 × 0.10 × 0.08
θ range, deg	2.74–27.56	2.57–26.46
no. of reflns collected	29 460	27 986
no. of indep reflns	8623 (<i>R</i> _{int} = 0.0679)	6548 (<i>R</i> _{int} = 0.0878)
abs corr	semiempirical from equivalents	semiempirical from equivalents
max. and min. transmn coeff	0.766 and 0.665	0.6910 and 0.4671
no. of params refined	453	327
GoF on <i>F</i> ²	1.033	1.061
<i>R</i> 1 ^a (<i>I</i> > 2 σ (<i>I</i>))	0.0405	0.0507
w <i>R</i> 2 ^b (all data)	0.1077	0.1214
peak and hole, e Å ⁻³	0.444 and -0.691	2.027 and -1.823

$$^a R1 = \sum ||F_o| - |F_c|| / \sum |F_o|. \quad ^b wR2 = \{ \sum [w(F_o^2 - F_c^2)^2] / \sum [w(F_o^2)^2] \}^{1/2}.$$

15.9 (d, ²*J*_{CPt} = 15 Hz, ¹*J*_{CP} = 19.2 Hz, P(CH₂CH₃)₃), 8.8 (³*J*_{CPt} = 22 Hz, P(CHHCH₃)₃), 8.1 (³*J*_{CPt} = 14 Hz, P(CH₂CH₃)₃), 4.5 (d, ²*J*_{CPt} = 67 Hz, ³*J*_{CP} = 6.0 Hz, CH₃); ²⁹Si{¹H} DEPT NMR (79.4 MHz, C₆D₆, 25 °C) δ -16.9 (¹*J*_{SIPt} = 1433 Hz, ²*J*_{SIP} = 208.8, 18.3 Hz); ³¹P{¹H} NMR (121.5 MHz, C₆D₆, 25 °C) δ 12.2 (¹*J*_{Ppt} = 1137 Hz, ²*J*_{PP} = 20.0 Hz), 11.7 (¹*J*_{Ppt} = 2132 Hz, ²*J*_{PP} = 20.0 Hz). Anal. Calcd for C₃₁H₄₆FeP₂PtSi₂: C 49.01, H 6.12. Found: C 49.17, H 6.20.

X-ray Crystallography. Selected crystal, data collection, and refinement parameters for **4a**, **4b**, **7a**, **8b**, **9**, **11**, **12**, and **15** are given in Tables 9, 10, and 11. Selected bond lengths and bond angles are given in Tables 1 (**4a**), 2 (**4b**), 3 (**7a**), 4 (**8b**), 5 (**9**), 6 (**11**), 7 (**12**), and 8 (**15**). Single-crystal X-ray diffraction data were collected at 150(1) K using a Nonius

Kappa-CCD diffractometer and monochromated Mo K α radiation (λ = 0.71073 Å). The data were integrated and scaled using the Denzo-SMN package.⁴¹ The SHELXTL/PC package was used to solve and refine the structures.⁴² Refinement was by full-matrix least-squares on *F*² using all data (negative intensities included). Hydrogen atoms were placed in calculated positions and included in the refinement in riding motion approximations.

The entire molecule of **4a** is disordered over two sites with occupancies 0.98/0.02. This was indicated by two large peaks

(41) Otwinowski, Z.; Minor, W. *Methods Enzymol.* **1997**, *276*, 307–326.

(42) Sheldrick, G. M. *SHELXTL/PC* V5.1; Bruker Analytical X-ray Systems: Madison, WI, 1997.

in the final difference Fourier map that had the same distance between them as Co(1) and Co(2). As a result, the cobalt atoms are refined with partial occupancies; the rest of the atoms are refined with full occupancy.

The $-\text{CH}_2-\text{CH}_2-$ backbone of the dmpe ligand in **10** is disordered over two sites with occupancies 0.81/0.19. Also, a difference Fourier map at an intermediate stage in the refinement revealed a volume of electron density that was associated with a severely disordered toluene molecule with 0.5 occupancy. The electron count contribution of this disordered solvent molecule was removed from the Fourier synthesis using the program SQUEEZE in PLATON.⁴³ Least-squares cycles run before and after this procedure showed no effect on the bond lengths and bond angles of the main molecule. The half molecule of toluene is included in the empirical formula.

CCDC-190309 (**4a**), CCDC-216383 (**4b**), CCDC-216378 (**7a**), CCDC-216382 (**8b**), CCDC-216379 (**9**), CCDC-216384 (**11**), CCDC-216381 (**12**), and CCDC-216380 (**15**) contain the supplementary crystallographic data for this paper. These data can be obtained free of charge via the Internet at www.ccdc.ca.

(43) Spek, A. L. *PLATON, A Multipurpose Crystallographic Tool*; Utrecht University: Utrecht, The Netherlands, 2003.

m.ac.uk/conts/retrieving.html (or from the Cambridge Crystallographic Data Centre, 12 Union Road, Cambridge CB2 1EZ, UK; fax: (+44) 1223-336-033; or e-mail: deposit@ccdc.cam.ac.uk).

Acknowledgment. We wish to acknowledge an NSERC postgraduate scholarship for W.Y.C. and A.B. and a PDF Scholarship for S.B.C.. I.M. is grateful to the NSERC Discovery Grants program for funding the research and to the University of Toronto for a McLean Fellowship (1997–2003), the Ontario Government for a PREA Award (1999–2003), and the Canadian Government for a Canada Research Chair. We also wish to thank Cory Jaska for supplying $[\text{Pt}(\text{PEt}_3)_4]$ and Dr. Timothy Burrow for collecting 2-D NMR data.

Supporting Information Available: Tables of atomic coordinates, bond lengths and bond angles, anisotropic displacement parameters, and hydrogen coordinates for compounds **4a**, **4b**, **7a**, **8b**, **9**, **11**, **12**, and **15**. This material is available free of charge via the Internet at <http://pubs.acs.org>.

OM030352P